Numerical Solutions for Compressible Flows

by

Sidra Shuja

A dissertation submitted in partial fulfillment of the requirements

for the degree of Master of Philosophy in Mathematics

Supervised by

Dr. Muhammad Asif Farooq

Department of Mathematics,

School of Natural Sciences (SNS),

National University of Sciences and Technology (NUST),

Islamabad, Pakistan.

August, 2015

National University of Sciences & Technology

M.Phil THESIS WORK

We hereby recommend that the dissertation prepared under our supervision by: SIDRA SHUJA, Regn No. NUST201361946MSNS78013F Titled: Numerical Solutions for Compressible Flows be accepted in partial fulfillment of the requirements for the award of **M.Phil** degree.

Examination Committee Members

1. Name: Dr. Meraj Mustafa Hashmi   Signature: _____

2. Name: Dr. Yousaf Habib   Signature: _____

3. Name: Dr. Adnan Maqsood   Signature: _____

4. Name: Dr. Masood KhaN   Signature: _____
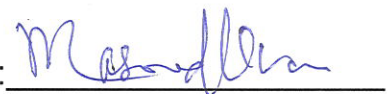
Supervisor's Name: Dr. Muhammad Asif Farooq   Signature: _____

_____   _____
Head of Department   28/8/15
                                                              Date

COUNTERSINGED

Date: 28/8/15   _____
                                                        Dean/Principal

بِسْمِ اللهِ الرَّحْمٰنِ الرَّحِيْمِ

In the name of Allah, the most beneficent, the most merciful.

Dedicated to

My parents, brother, and the best friend

Abstract

In this thesis, numerical solutions of compressible fluid are developed for compressible flow problems. In the first part, the variable fluid properties have been studied for the Sakiadis flow. This work is extended for the case of stretching sheet. The arising non-linear partial differential equations (PDEs) are reduced into the system of non-linear ordinary differential equations (ODEs) by using similarity transformations. Constant fluid properties and temperature-dependent viscosity are considered for the solution which is obtained by using the built-in solver *bvp4c* of MATLAB and are compared with the shooting method using a fifth order Runge-Kutta Method.

The momentum boundary layer is seen to grow in the direction of motion of the surface. This characteristic is not observed when a semi-infinite flat plate moves through a quiescent fluid and the boundary layer grows in the direction opposite to that in which the plate is moving. Heat is transferred by the mechanism of conduction, convection or radiation. In the present work, convection (free) is the source of heat transfer due to temperature difference between surface and an ambient fluid and conservation equations are used to find its solution.

In the second part of the thesis, the compressible Euler equation has been solved. For time integration, we use explicit Euler method and for space discretization, the first order Lax-Friedrich and local Lax-Friedrich schemes are used. For the inviscid compressible flow, we test the case of Shock tube problem. Results for different variables are presented.

Acknowledgements

Contents

List of Figures

1

List of Tables

Chapter 1

Introduction

1.1   Literature Review

The study of laminar compressible flow over moving flat surface as well as over a stretching sheet is taken into account in the present work. The motion of the surface induces a motion in the adjacent fluid. Sakiadis was probably the first person who solved the problem of forced convection over an isothermal moving plate. He derived the basic differential and integral momentum equations for boundary layer on both continuous and solid surfaces [1,2]. As Sakiadis considered an ambient fluid over a moving continuous surface, his boundary layer was different from that of Blasius who considered a flow over a fixed flat plate [3]. Since that time researchers have considered the problem for various situations ranging from flat surface to cylinder. Solutions that included mass transfer, varying plate velocity, varying plate temperature, fluid injection and fluid suction at the plate have been obtained.

Most of the studies for the ambient fluid is carried out by considering constant physical properties of fluid which provides parabolic velocity profile for laminar flow and may introduce severe error as described by Ioan Pop et al. [4]. However, in reality all physical properties involved in the condition are dependent on temperature [5]. Andersson and Aarseth [6] revised the Sakiadis flow by considering variable viscosity of the fluid on a moving flat surface. In Chapters 2 and 3 of this work,

the effects of temperature-dependent viscosity are considered to accurately predict the flow as viscosity changes significantly with temperature [6]. Takhar et al. [7] assumed that dynamic viscosity, density, and thermal conductivity exhibited power law variation with absolute temperature. Temperature-dependent viscosity has not received much attention despite its importance. In current work, Chapters 2 and 3 deals with the constant and temperature-dependent viscosity over steadily flat and stretching surface, respectively. Unlike previous works, chapter 4 presents the solution of the compressible Euler equation.

1.2   Basic Definitions and Concepts

1.2.1   Viscosity

A measure of fluid resistance to flow is called *dynamic viscosity* μ. In simple words, viscosity refers to thickness. For example, water is thin, have a low viscosity and can flow easily while honey is thick and have a high viscosity so its movement is slow. The ratio of dynamic viscosity to density is called *kinematic viscosity*. It is also called momentum diffusivity.

It is denoted by ν and expressed as

$$\nu = \frac{\mu}{\rho}.$$

Viscosity varies with temperature. Honey and syrups flow more readily when heated. In general, the viscosity of a simple liquid decreases with increasing temperature and increases with decreasing temperature. Engine oil and hydraulic fluids thicken on cold days and significantly affect the performance of machineries in winters. As temperature increases, the average speed of the molecules in a liquid increases. Thus, the average intermolecular forces decrease and the gases get thicker with the rise of temperature. The viscosity of gases increases as temperature increases. This is due to the increase in the frequency of intermolecular collisions at higher temperatures. Ostwald viscometer is a common device to measure the viscosity of liquids.

1.2.2 Newtonian Fluid

Fluids for which the rate of deformation is proportional to the shear stress are called Newtonian fluids [8]. Mathematically, it can be described as

$$\tau = \mu \frac{du}{dy},$$

the proportionality constant μ is the coefficient of dynamic viscosity and du/dy is the velocity gradient also known as the rate of deformation.

1.2.3 Thermal Conductivity

A physical property of fluid that mediates diffusion of heat through a substance is called thermal conductivity. It is denoted by k.

1.2.4 Boundary Layer Flows

When fluid flows over a solid surface, the layer of the fluid particles in immediate contact to the surface attaches to it, this is called the *no-slip condition*. This results in generation of boundary layer in the vicinity of surface. That thin layer is called *momentum boundary layer* in which strong viscous effects exist due to large velocity gradients. The thickness of this region between the surface and the free-stream velocity increases in the direction of flow. The flow past a surface is divided into two regions: a region far from the surface of the body in which the effects of such fluid properties as viscosity and thermal conductivity are negligible and a region close to the surface where these properties are not negligible. The flow outside the boundary layer is inviscid and Euler equation is applied there.

The pressure distribution throughout the boundary layer in the direction normal to the surface remains constant. Also note that strong gradients of velocity and temperature occur in the boundary layer [4].
Unlike momentum boundary layer, *thermal boundary layer* is defined as a region due to the transfer of heat between the surface and fluid and characterized by heat fluxes
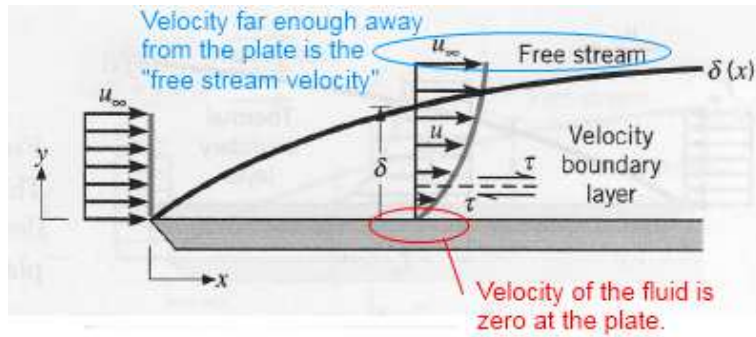
Figure 1.1: Momentum boundary layer [9].

and temperature gradients. Its thickness also increases in the direction of flow. The velocity and thermal boundary layers will not be identical except when $Pr = 1$. Additional influencing factors change the thickness of the thermal boundary layer as compared to the thickness of the velocity boundary layer at any point [10].
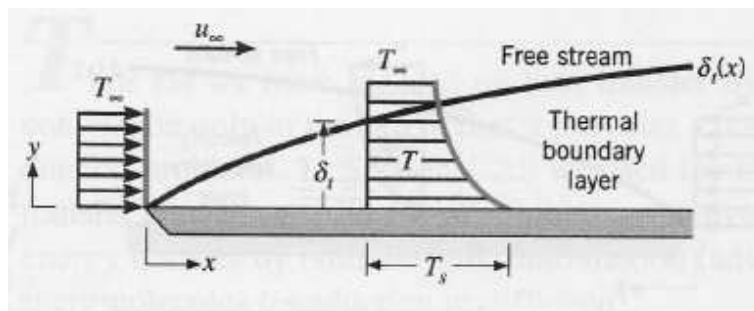
Figure 1.2: Thermal boundary layer [9].

6

1.2.5 Compressible Flow

It is defined as a flow in which density varies. It is in contrast to incompressible flow where the density is assumed to be constant. Liquids have a low level of compressibility (for water 5×10^{-10} m^2/N at 1 atm) while gases have a high level of compressibility (for air 10^{-5} m^2/N) [11]. Compressible flows are also classified according to the value of dimensionless Mach number, Ma, which is defined as

$$Ma = \frac{u}{c}$$

where u is a velocity of the fluid and c is the speed of the sound.

1.2.6 Steady Flow

Fluid flows also show the property of steady or unsteady flow. In steady flow, the fluid properties, such as temperature, pressure, density etc, in the control volume don't change with time [12]. Mathematically

$$\frac{\partial u}{\partial t} = \frac{\partial p}{\partial t} = \frac{\partial \rho}{\partial t} = \frac{\partial T}{\partial t} = 0.$$

For instance, flow around an aeroplane that is moving with a constant velocity is steady.

1.2.7 Laminar Flow

Two types of motions are observed in fluid dynamics. The smooth motion of real fluid in parallel layers (laminae) with no macroscopic mixing is called a laminar flow. The momentum or heat transfer happens at the molecular level and velocity at any point remains steady (i.e. a smooth function of time). The laminar flow occurs when:

1. the liquid viscosity is relatively high.

2. Liquid velocity is below the certain level [13].

3. Reynolds number is low.

1.2.8   Turbulent Flow

The three-dimensional and random or chaotic motion of individual particles due to
a high flow rate is called a turbulent flow. The velocity at any point varies with
respect to a mean value [11]. Unlike laminar flow, the turbulent flow is easy to find
in nature.
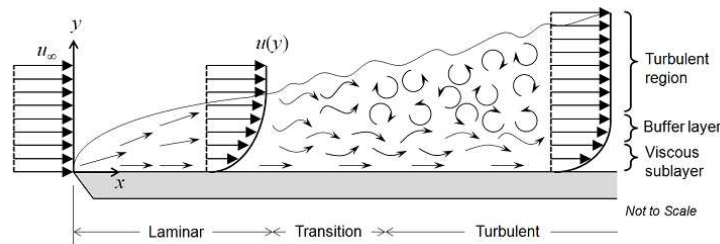
Figure 1.3: Laminar and turbulent flows [9].

1.2.9   Prandtl Number

The relative thickness of velocity and thermal boundary layers are defined by the
parameter Prandtl number, which is a dimensionless quantity. Mathematically,

$$Pr = \frac{\nu}{\alpha} = \frac{\mu c_p}{k},$$

where μ, c_p, and k are dynamic viscosity, specific heat at constant pressure and
thermal conductivity, respectively.

Prandtl number of gases are about 1, which indicates that both momentum and heat
dispel (or dissipate) through fluid at approximately the same rate. When $Pr \ll 1$,
thermal diffusivity dominates and when $Pr \gg 1$, momentum diffusivity dominates.
Prandtl number controls the relative thickness of momentum and thermal boundary

layers in case of heat transfer.

Few values of Prandtl number for different fluids are given as

Pr= $0.16 - 0.17$ for mixture of Noble gases.

Pr= 0.71 for air at room temperature.

Pr= 10 for water at temperature $20\,^{\circ}\text{C}$.

Pr= 13.4 for sea-water at $0\,^{\circ}\text{C}$.

Pr= $50 - 2000$ for oils.

1.3 Governing Equations of Fluid Dynamics

The governing equations form basic principle in fluid dynamics. These are conservation equations of mass, momentum, and energy. They can be expressed in general terms as follows:

1. The mass of fluid is conserved.

2. According to Newton's second law, the rate of change of momentum equals the sum of the forces on fluid particles [14].

3. The rate of change of energy is equal to the sum of the rate of the heat addition to and the rate of work done on a fluid particle [14]. This is known as the first law of thermodynamics.

1.3.1 Continuity Equation

The continuity equation states that the mass of the fluid is conserved. Let us take a fixed surface S in the fluid and V is its control volume. The rate of flow of mass into V is

$$- \int_s (\rho \mathbf{v}).dS.$$

The negative sign shows that mass flux $\rho \mathbf{v}$ is entering in V. The rate of increase of mass flow is

$$\frac{d}{dt} \int_V \rho \, dV.$$

The integral and derivative can be interchanged because of constant volume V.

$$\int_V \frac{\partial \rho}{\partial t} \, dV.$$

As mass is conserved, the conservation equation can be written as

$$\int_V \frac{\partial \rho}{\partial t} \, dV = - \int_S (\rho \mathbf{v}).dS. \qquad (1.3.1)$$

By using the divergence theorem, above equation becomes

$$\int_V \left(\frac{\partial \rho}{\partial t} + \nabla.(\rho \mathbf{v}) \right) dV = 0.$$

We assume that integrand is continuous, therefore, the above equation can be written as

$$\frac{\partial \rho}{\partial t} + \nabla.(\rho \mathbf{v}) = 0. \qquad (1.3.2)$$

The equation is valid for compressible flow.

For steady flow

$$\frac{\partial \rho}{\partial t} = 0.$$

This equation is still valid for compressible flow and equation (1.2.2) can be written as

$$\nabla.(\rho \mathbf{v}) = 0. \qquad (1.3.3)$$

This is called a continuity equation or conservation equation of mass.

1.3.2 Conservation of Momentum

We apply Newton's second law for developing principle of conservation of momentum. This law is applied to the moving fluid element which states that the rate of change of momentum of fluid mass is equal to the net external forces acting on the mass [15]. The moving fluid element experiences a force. There are two sources of that force.

1. **Body forces**: These forces act at a distance on the mass of the fluid element. For example, gravitational, electric and magnetic forces.

2. **Surface forces**: It acts directly on the surface of the fluid element. These forces are due to

(a) the pressure distribution acting on the surface, imposed by the outside fluid surrounding the fluid element,

(b) the shear and normal stress distributions acting on the surface due to viscosity [16].

The rate of increase of momentum in volume V is equal to the sum of the

1. rate of change of momentum through S
2. total body force per unit mass acting on fluid element within V
3. total surface force per unit area acting on S [17].

The mass per unit volume is ρ and ith component of momentum is ρv_i. The rate of momentum through S is

$$-\int_s \mathbf{n}.\rho v_i \, \mathbf{v} \, dS,$$

The negative sign shows an inward flow. $\mathbf{n}$ is a normal to the surface.

Also the rate of change of momentum of the mass contained in volume V is

$$\frac{d}{dt} \int_V \rho v_i \, dV.$$

11

Let the resultant body force per unit mass acting on fluid element is denoted by $\mathbf{f}$. The net external body force acting on a mass of volume V is given by

$$\int_V \rho \mathbf{f}_i \, dV.$$

Similarly, let the resultant surface force per unit area is denoted by $\mathbf{P}$, then the net external surface force acting on the surface S containing volume V is

$$\int_s \mathbf{P} \, dS.$$

Thus the equation of motion for the fluid is

$$\frac{d}{dt} \int_V \rho v_i \, dV = -\int_s \mathbf{n}.\rho v_i \, \mathbf{v} \, dS + \int_V \rho \mathbf{f}_i \, dV + \int_s \mathbf{P} \, dS.$$

There are nine components of stress at any given point; three normal components and six shear components on each coordinate plane. The surface force $\mathbf{P}$ is related to stress tensor σ_{ij} because three stress components acting on the surface S are σ_{ii}, σ_{ij} and σ_{ik} in x, y and z directions. The unit normal vector acting on this surface is $\hat{n}_i$, then surface force will be given by

$$P_j = \sigma_{ij} \hat{n}_i.$$

The above mathematical equation can be written as

$$\frac{d}{dt} \int_V \rho v_i \, dV = -\int_s \mathbf{n}.\rho v_i \, \mathbf{v} \, dS + \int_V \rho \mathbf{f}_i \, dV + \int_s \sigma_{ij} \hat{n}_i \, dS.$$

The surface integral on the right hand side may be converted to volume integral by using Gauss's divergence theorem. This leads to

$$\int_V \left(\frac{\partial}{\partial t} \rho v_i\right) dV = \int_V \left(-\nabla.\rho v_i \, \mathbf{v} + \rho \mathbf{f}_i + \frac{\partial}{\partial x_j} \sigma_{ij}\right) dV.$$

Here we assume that V is arbitrary and integrand is smooth. Therefore, we have

$$\frac{\partial}{\partial t}(\rho v_i) = -\nabla.\rho v_i \, \mathbf{v} + \rho \mathbf{f}_i + \frac{\partial}{\partial x_j} \sigma_{ij}.$$

12

By using the identity

$$\nabla.(vw) = v.(\nabla w) + w.(\nabla v)$$

and continuity equation, the above equation expressing conservation of momentum becomes

$$\rho\frac{\partial v_i}{\partial t} = -\rho v_i.\nabla\mathbf{v} + \rho\mathbf{f}_i + \frac{\partial}{\partial x_j}\sigma_{ij}. \tag{1.3.4}$$

1.3.3 Conservation of Energy

The first law of thermodynamics deals with the conservation of energy. It states that the rate of energy equals the sum of rate of heat addition to and work done on fluid particles. Heat is transferred from a system at the higher temperature to one at the lower temperature as a result of temperature difference between the two systems.

Consider an arbitrary mass of fluid enclosed in volume V. The total energy of the mass per unit volume is

$$\rho e + \frac{1}{2}\rho u^2$$

The rate of total energy contained in volume V is

$$E = \int_V (\rho e + \frac{1}{2}\rho u^2)\, dV,$$

here e is the internal energy per unit mass and $\frac{1}{2}u^2$ is the kinetic energy per unit mass.

The work done by the two external forces (surface and body forces) on fluid is the product of velocity and force vectors. The magnitude of surface force (stress) per unit area is represented by vector $\mathbf{P}$. Then total work due to these forces will be

$$\int_s \mathbf{u}.\mathbf{P}\, dS$$

where S is the surface (boundary) enclosing volume V.

Similarly, the magnitude of body force per unit mass is vector $\mathbf{f}$. Then the total

13

work done the fluid particle due to body force is

$$\int_V \mathbf{u}.\rho\mathbf{f}\,dV.$$

Let heat flux adding to the control volume is vector $\mathbf{q}$. The quantity of heat flux per unit time per unit surface area is $\mathbf{q}.\mathbf{n}$.

Thus the net amount of heat per unit area is

$$\int_s \mathbf{q}.\mathbf{n}\,dS$$

where $\mathbf{n}$ is the unit outward normal.

The statement of law can be written in analytical form [15] as

$$\frac{d}{dt}\int_V (\rho e + \frac{1}{2}\rho u^2)\,dV = \int_V \rho\vec{f}.\mathbf{u}\,dV + \int_s \mathbf{P}.\mathbf{u}\,dS - \int_s \mathbf{q}.\mathbf{n}\,dS.$$

Using Reynolds transport theorem, the above equation can be written as

$$\int_V \frac{\partial}{\partial t}(\rho e + \frac{1}{2}\rho u^2)\,dV + \int_s (\rho e + \frac{1}{2}\rho u^2)(\mathbf{u}.\mathbf{n})\,dS = \int_V \rho\mathbf{f}.\mathbf{u}\,dV + \int_s \mathbf{P}.\mathbf{u}\,dS - \int_s \mathbf{q}.\mathbf{n}\,dS.$$
$$(1.3.5)$$

It can be explained by the theorem as, "the total time derivative of an integral with time-dependent limits equals the integral of the partial time derivative of the integrand plus a term that accounts for the motion of the integration boundary" [12]. Using Gauss's theorem, the surface integral is converting into volume integral.

$$\int_s (\rho e + \frac{1}{2}\rho u^2)(\mathbf{u}.\mathbf{n})\,dS = \int_V \nabla.(\rho e + \frac{1}{2}\rho u^2)\mathbf{u}\,dV$$
$$= \int_V \frac{\partial}{\partial x_j}(\rho e + \frac{1}{2}\rho\mathbf{u}_i.\mathbf{u}_i)\mathbf{u}_j\,dV \qquad (1.3.6)$$

Similarly we know that force vector P is related to tensor vector by the equation $P_j = \sigma_{ij}n_i$. Then

$$\int_s \mathbf{P}.\mathbf{u}\,dS = \int_s \sigma_{ij}n_i u_j\,dS$$
$$= \int_V \frac{\partial}{\partial x_j}\sigma_{ij}u_j\,dV. \qquad (1.3.7)$$

14

And

$$\int_s \mathbf{q}.\mathbf{n}\, dS = \int_s \mathbf{q}_j.\mathbf{n}_j\, dS$$

$$= \int_V \nabla.\mathbf{q}\, dV = \int_V \frac{\partial q_i}{\partial x_i}\, dV. \tag{1.3.8}$$

Substituting equations (1.2.6)-(1.2.8) in Eq. (1.2.5), expression for conservation of energy becomes

$$\int_V (\frac{\partial}{\partial t}(\rho e + \frac{1}{2}\rho u^2) + \frac{\partial}{\partial x_i}(\rho e + \frac{1}{2}\rho \mathbf{u}_j.\mathbf{u}_j)u_i)\, dV = \int_V (\rho \mathbf{f}_j \mathbf{u}_j + \frac{\partial}{\partial x_i}\sigma_{ij}u_j - \frac{\partial q_i}{\partial x_i})\, dV.$$

If integrand vanishes at every point in space, we obtain the differential equation of conservation of energy.

$$\frac{\partial}{\partial t}(\rho e + \frac{1}{2}\rho u^2) + \frac{\partial}{\partial x_i}(\rho e + \frac{1}{2}\rho \mathbf{u}_j.\mathbf{u}_j)\mathbf{u}_i = \rho \mathbf{f}_j \mathbf{u}_j + \frac{\partial}{\partial x_i}\sigma_{ij}\mathbf{u}_j - \frac{\partial q_i}{\partial x_i}.$$

$$\tag{1.3.9}$$

1.4 Compressible Euler Equations

The compressible Euler equations are comprised of continuity, momentum and energy equations. They are used in applications where viscosity is negligible. As we are studying compressible flow in this work, compressible Euler equations are equations for perfect fluids when heat conduction, viscosity, and mass diffusion are neglected. The Euler equations are mathematically a set of three hyperbolic partial differential equations. Hyperbolic partial differential equations typically arise in wave motion. Here we consider the compressible Euler equations in conservative form which is generally non-linear.

We use a fixed region of space called a control volume in which both mass and energy can cross the boundary of the control volume [10]. According to the conservation law, the rate of change of total amount of material contained in a control volume V is equal to the flux of that material in a closed surface S [18]. Let $\rho(x,t)$ is a density

of the material (kg/m^3) at time t and at point x. Then the total mass inside V is

$$\int_V \rho \, dV$$

The rate of change of total mass can be written as

$$\frac{d}{dt} \int_V \rho \, dV$$

The flow of quantity has size and direction and is called flux which is a vector quantity. Let flux vector is represented by $\mathbf{F(x,t)}$. For conserved mass, the only flow at a particular time which affects the total mass is the flow through its boundary surface S in V at that time [19]. We consider only the values of $\mathbf{F}$ at points on the boundary of V where $\mathbf{F}$ can be in any direction. Hence for inward flux, $\mathbf{F}$. $\mathbf{n}$ is the normal component of $\mathbf{F}$ at the boundary of V.

A total flux through a surface element dS of the boundary surface S is given by

$$- \int_s (\mathbf{F}.\mathbf{n}) \, dS$$

The negative sign shows the inward flux. Then conservation law is given by

$$\frac{d}{dt} \int_V \rho \, dV = - \int_s (\mathbf{F}.\mathbf{n}) \, dS.$$

Taking d/dt inside the integral and applying Gauss's divergence theorem, we obtain

$$\int_V \left(\frac{\partial \rho}{\partial t} + \nabla \mathbf{F} \right) dV = 0.$$

If integrand is continuous, it must vanish everywhere in the domain. Thus we get the conservation equation in the form

$$\frac{\partial \rho}{\partial t} + \nabla \mathbf{F} = 0, \tag{1.4.1}$$

which is the general form of compressible Euler equation in conservative form. The components of $\rho = (\rho_1, \rho_2, ..., \rho_n) \in \mathbb{R}^n$ are conserved and components of the function $\mathbf{F} = (f_1, f_2, ..., f_n) : \mathbb{R}^n \to \mathbb{R}^n$ are corresponding fluxes.

1.5 Numerical Methods

BVPs are much harder to solve than IVPs and any solver might fail. A solution to the initial value problem always exists and is unique. Unlike initial value problem (IVP), boundary value problem (BVP) specifies equations at more than one point and may or may not have finite solutions. In this work, numerical algorithms are used to solve nonlinear boundary value problems and to find the unknown values of shock waves. These methods are listed here.

1.5.1 Shooting Method

Shooting method can be used for both linear and non-linear equations. The basic algorithm of the shooting method is the supposition of trial value. The solution begins at one end of the boundary value problem, and shoot to the other end like a cannon-ball (reaching its target under the influence of gravity) with an initial value solver until the boundary condition at the other end converges to its true value. The advantage of the shooting method is that the speed and adaptivity of methods for initial value problems is considered.

For a boundary value problem of a third-order differential equation, consider
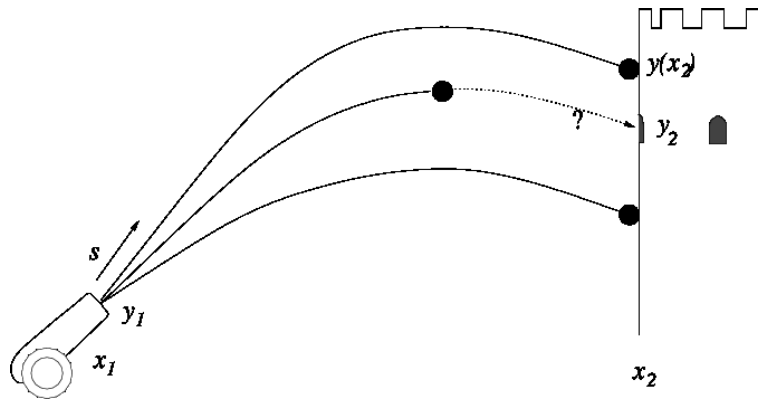
Figure 1.4: Multiple shots from a canon to strike the target.

$$y''' = f(x, y, y', y''), \quad \forall \, a \leq x \geq b,$$
$$y(a) = \alpha, \quad y'(a) = \gamma, \quad y'(b) = \beta \tag{1.5.1}$$

where α, β and γ are the given constants.

Consider the initial guess is s_0 that finds the solution of the derivative $y''(a)$. Then

$$y'''(x, s) = f(x, y(x, s), y'(x, s), y''(x, s)), \quad \forall \, a \leq x \geq b,$$
$$y(a) = \alpha, \quad y'(a) = \gamma, \quad y'(b) = \beta, \quad y''(a, s) = s_0. \tag{1.5.2}$$

Differentiate Eq. (1.5.2) with respect to s and we get

$$\frac{\partial y'''}{\partial s} = \frac{\partial f}{\partial x}(x, y(x, s), y'(x, s), y''(x, s))\frac{\partial x}{\partial s} + \frac{\partial f}{\partial y}(x, y(x, s), y'(x, s), y''(x, s))\frac{\partial y}{\partial s} +$$
$$\frac{\partial f}{\partial y'}(x, y(x, s), y'(x, s), y''(x, s))\frac{\partial y'}{\partial s} + \frac{\partial f}{\partial y''}(x, y(x, s), y'(x, s), y''(x, s))\frac{\partial y''}{\partial s}.$$

Let $z(x, s) = \frac{\partial y}{\partial s}(x, s)$, then

$$z'' = \frac{\partial f}{\partial y}(x, y, z, z')z + \frac{\partial f}{\partial y'}(x, y, z, z')z' + \frac{\partial f}{\partial y''}(x, y, z, z')z'', \quad \forall \, a \leq x \geq b,$$
$$z(a) = 0, \quad z'(a) = 0, \quad z''(a) = 1. \tag{1.5.3}$$

To choose value of s_0 such that

$$y(b, s) - \beta = 0$$

then

$$s_0 = y'(a) = \frac{y(b) - y(a)}{b - a}$$

18

$$s_0 = \frac{\beta - \alpha}{b - a}$$

Newton Raphson Method is used to approximate the solution of $y(b, s) - \beta = 0$ and find a next guess s_{k+1}.

$$s_{k+1} = s_k - \frac{y'(b, s_k) - \beta}{z(b, s_k)} \qquad (1.5.4)$$

Eq. (1.5.3) is converted into a first order ordinary differential equation by replacing z' by another variable. Then a first order ordinary differential equation can be solved by Runge Kutta method. The process will stop until the error is $|\beta - y'(b, s_k)| \leq$ Tolerance value.

1.5.2 Runge Kutta Method

The Runge Kutta methods are a family of a single step and include both implicit and explicit iterative methods. As an explicit RK method of fifth order is used in the present work, so it is described here.

Consider an initial value problem

$$\frac{dy}{dx} = f(x, y), \qquad y(0) = y_0$$

We integrate the general ODE from x_n to x_{n+1}

$$y_{n+1} = y_n + \int_{x_n}^{x_{n+1}} f(\tau, y(\tau)) d\tau$$

By replacing the integral by quadrature method, we obtain

$$y_{n+1} = y_n + \sum_{j=1}^{v} b_j f(x_n + c_j h, y_n + h c_j k_j), \quad n = 0, 1, 2, \ldots$$

19

where k_j are increments based on the slope and c_j are nodes at which the values of y are unknown.

$$k_1 = hf(x_n, y_n),$$
$$k_2 = hf(x_n + c_2h, y_n + a_{21}k_1(x_n, y_n))$$
$$\vdots$$
$$k_n = hf(x_n + c_vh, y_n + \sum_{m=1}^{v-1} a_{v,m}k_m).$$

To specify a fifth order RK, we need to provide the integer v (the number of stages), and the coefficients c_v, $a_{v,m}$, and b_j. These data are usually obtained from a Butcher tableau.

Hence for fifth order RK method, increments $k_1, k_2, k_3, k_4, k_5, k_6$ are given by

$$k_1 = hf(x_n, y_n),$$

$$k_2 = hf(x_n + \tfrac{h}{5}, y_n + \tfrac{1}{5}k_1) \tag{1.5.5}$$

$$k_3 = hf(x_n + \tfrac{3h}{10}, y_n + \tfrac{3}{40}k_1 + \tfrac{9}{40}k_2) \tag{1.5.6}$$

$$k_4 = hf(x_n + \tfrac{3h}{5}, y_n - \tfrac{3}{10}k_1 - \tfrac{9}{10}k_2 + \tfrac{6}{5}k_3) \tag{1.5.7}$$

$$k_5 = hf(x_n + h, y_n - \tfrac{11h}{54}k_1 + \tfrac{5}{2}k_2 - \tfrac{70}{27}k_3 + \tfrac{35}{27}k_4) \tag{1.5.8}$$

$$k_6 = hf(x_n + \tfrac{7h}{8}, y_n - \tfrac{1631}{55296}k_1 + \tfrac{175}{512}k_2 + \tfrac{575}{13824}k_3 + \tfrac{44275}{110592}k_4 + \tfrac{253}{4096}k_5) \tag{1.5.9}$$

and general form of equation is

$$y_{n+1} = y_n + (\frac{37}{378}k_1 + \frac{250}{621}k_3 + \frac{125}{594}k_4 + \frac{512}{1771}k_6) \tag{1.5.10}$$

1.5.3 Lax Friedrichs Methods

Lax-Friedrichs is a finite difference method which is used for numerically solving hyperbolic partial differential equations. It is a first order in time, explicit in time, consistent, and conservative method.

The conservative hyperbolic differential equation in nonlinear form can be written as

20

$$\frac{\partial U}{\partial t} + \frac{\partial F}{\partial x} = 0, \tag{1.5.11}$$

As Lax-Fedrich is based on Forward-Time, Central-Space method (FTCS), we expand Taylor's series upto second order on grid points $x_j - \Delta x$ and $x_j + \Delta x$.

$$F(x_j - \Delta x, t^n) = F(x_j, t^n) - \frac{\partial F}{\partial x}(x_j, t^n)\Delta x + \frac{1}{2}\frac{\partial^2 F}{\partial x^2}(x_j, t^n)\Delta x^2 + \mathcal{O}(\Delta x^3),$$

$$F(x_j + \Delta x, t^n) = F(x_j, t^n) + \frac{\partial F}{\partial x}(x_j, t^n)\Delta x + \frac{1}{2}\frac{\partial^2 F}{\partial x^2}(x_j, t^n)\Delta x^2 + \mathcal{O}(\Delta x^3),$$

After substrating these two expressions, we obtain

$$\frac{\partial F}{\partial x}(x_j, t^n) = \frac{F(x_j + \Delta x, t^n) - F(x_j - \Delta x, t^n)}{2\Delta x} \tag{1.5.12}$$

which provides us with a central difference formula. In order to discreitze time, we apply forward Euler method. Letting $U(j\Delta x, n\Delta t)$, forward Euler method is given as

$$\frac{\partial U}{\partial t} = \frac{U(x_j, t^{n+1}) - U(x_j, t^n)}{\Delta t}. \tag{1.5.13}$$

Substituting Eqs. (1.5.12) and (1.5.13) in Eq. (1.5.11), we finally obtain the form of Lax-Friedrich method.

$$U_j^{n+1} = U_j^n - (\Delta t/2\Delta x)(F_{j+1}^n - F_{j-1}^n). \tag{1.5.14}$$

A numerical flux can be defined as

$$F(U_{j+1}^n, U_j^n) = \frac{1}{2}(F(U_{j+1}^n) + F(U_j^n)) - \frac{\Delta x}{2\Delta t}(U_{j+1}^n - U_j^n). \tag{1.5.15}$$

The stability and convergence of finite difference method is checked by the condition

21

known as Courant-Friedrich-Lax condition (CFL). CFL is a necessary but not a sufficient condition. If it is violated then method can't be convergent. If it is satisfied, still a proper stability analysis is required to check the convergence. It is defined by the following condition

"The full numerical domain of dependence must contain the physical domain of dependence."

Any method that violates this condition is unstable and causes error. For one dimensional case, CFL is defined as

$$CFL = \max(|(u+a)|)\Delta t / \Delta x \leq 1. \qquad (1.5.16)$$

LFM can be improved by replacing $\frac{\Delta x}{2\Delta t}$ by $\max(|(F'(U_{j+1}), F'(U_j))|)$. This method is called Rusanov's method or local Lax-Friedrich Method. Lax-Friedrich Method converges to the true solution as $\Delta x \to 0$ and $\Delta t \to 0$, provided CFL is satisfied. LFM is a first order accurate in space and time.

1.5.4 $bvp4c$

A programming in MATLAB requires a guess for solving BVP. $bvp4c$ is one such effective solver for solving BVP. As the shooting method is not as robust as finite difference or collocation methods, we have also used $bvp4c$. It is a collocation method and starts solution with initial guess supplied at initial mesh points. A step-size is also changed to obtain the specified accuracy. As BVPs are much difficult to solve, in this respect, $bvp4c$ is an effective solver. Contrary to the shooting method, the solution is approximated over the whole interval and boundary conditions are considered all the time [36].

Chapter 2

Numerical Solution of Sakiadis Flow with Variable Fluid Properties

2.1 Introduction

This chapter is the review work of Andersson and Aarseth [6]. A study of boundary layer over a continuous solid surfaces has attracted little attention from researchers despite its increasing industrial applications which include the cooling of an infinite metallic plate in a cooling bath, the boundary layer along material handling conveyers, the aerodynamic extrusion of plastic sheets, the boundary layer along a liquid film in condensation processes, paper and glass production, metal spinning, drawing plastic films and polymer extrusion. The behaviour of boundary layer flow on continuous solid surfaces was first examined by Sakiadis [1, 2]. Sakiadis used Blasius transformation to reduce partial differential equations into ordinary differential equations. The ordinary differential equation was identical to that obtained by Blasius [3] but the boundary conditions and velocity profile were different. Solutions have been appeared including mass transfer, varying plate velocity, varying plate temperature, fluid injection and fluid suction at the plate [20]. Tsou et al. [21] extended the work of Sakiadis by combining analytical and experimental study

23

of momentum and temperature fields on a continuous moving surface and found an excellent agreement between experimental measurements and analytical predictions. Andersson has considered the influence of variable fluid properties and for this he introduced a new similarity transformation inspired by the Howarth-Dorodnitsyn transformation [6].

2.2   Mathematical Formulation

Consider the laminar flow of a Newtonian fluid that is driven by a moving flat surface. T_0 is a constant temperature of an ambient fluid and T_w is a constant temperature of the continuous surface. Let the flat surface is moving with a constant speed U in the x-direction while y-axis is perpendicular to the surface. It is observed that momentum and thermal boundary layer thicknesses develop and grow in the direction of the flow. For compressible flow, energy equation is also considered along continuity and momentum equations.

The velocity and temperature inside the momentum and thermal boundary layers are governed by the conservation equations for mass, momentum and energy as follows:

$$\frac{\partial}{\partial x}(\rho u) + \frac{\partial}{\partial y}(\rho v) = 0, \tag{2.2.1}$$

$$u\frac{\partial u}{\partial x} + v\frac{\partial u}{\partial y} = \frac{1}{\rho}\frac{\partial}{\partial y}\left(\mu\frac{\partial u}{\partial y}\right), \tag{2.2.2}$$

$$u\frac{\partial T}{\partial x} + v\frac{\partial T}{\partial y} = \frac{1}{\rho c_p}\frac{\partial}{\partial y}\left(\frac{k\partial T}{\partial y}\right), \tag{2.2.3}$$

here u represents a velocity component along x-axis and v a velocity component along y-axis, T is taken as a temperature inside the boundary layer, ρ is the density of the fluid , μ is the dynamic viscosity, k is the thermal conductivity and c_p is the specific heat at a constant pressure. Pressure gradient is neglected in equations

(2.2.1), (2.2.2), and (2.2.3). The boundary conditions for the given problem are

$$u = U, \quad v = 0, \quad T = T_w \text{ at } y = 0,$$
$$u \to 0 \text{ as } y \to \infty, \quad T \to T_0 \text{ as } y \to \infty. \tag{2.2.4}$$

The similarity transformation may be defined as a rule for combining two independent variables x and y into ODEs and are used to transform Eqs. (2.2.1), (2.2.2) and (2.2.3) into ODEs along with boundary conditions. We introduce the following dimensionless variables

$$\eta = \sqrt{\frac{U}{a\nu_0 x}} \int \frac{\rho}{\rho_0} dy, \qquad \psi = \rho_0 \sqrt{a\nu_0 x U} f(\eta), \tag{2.2.5}$$

$$\theta(\eta) = \frac{T - T_0}{T_w - T_0}, \tag{2.2.6}$$

here ρ_o and ν_o are the values of ambient fluid at temperature T_0 and a is a dimensionless positive constant. Here η is a similarity variable and $f(\eta)$ and $\theta(\eta)$ are new dependent variables. It is emphasized that the transformation (2.2.6) exists only if $T_w \neq T_0$. In the special case $T_w = T_0$, the trivial solution $T(x, y) = T_0$ solves the energy Eq. (2.2.3) subject to the boundary conditions in Eq. (2.2.4). Here f is a reduced stream function that depends on η.

It is important to note that θ is positive for gases and negative for liquids when $(T_w - T_0)$ is positive as mentioned in refs [4] and [22].

We choose a stream function $\psi(x, y)$ by

$$\rho u = \frac{\partial \psi}{\partial y}, \qquad \rho v = -\frac{\partial \psi}{\partial x} \tag{2.2.7}$$

25

Obviously the above equation satisfies mass conservation equation (2.2.1). Substituting all above equations in Eqs. (2.2.1), (2.2.2), and (2.2.3) transform them into following ordinary differential equations:

$$\left(\frac{2}{a}\right)\left(\frac{\rho\mu}{\rho_0\mu_0}f''\right)' + f(\eta)f''(\eta) = 0. \tag{2.2.8}$$

$$\left(\frac{\rho k}{\rho_0 k_0}\theta'(\eta)\right)' + \frac{aPr_0}{2}\theta'(\eta)f(\eta) = 0. \tag{2.2.9}$$

In the transformed energy equation (2.2.9), the Prandtl number has been assumed constant across the boundary layer [6]. Pr_0 is given by $Pr_0 = \mu_o c_p / k_0$. Thus transformed boundary conditions are

$$f(0) = 0, \quad f'(0) = 1, \quad \theta(0) = 1 \quad \text{at} \quad \eta = 0,$$
$$f' \to 0, \quad \theta \to 0 \quad \text{as} \quad \eta \to \infty. \tag{2.2.10}$$

An exact similarity exists when all coefficients in Eqs. (2.2.8) and (2.2.9) are either constants or only functions of η [6]. The requirement for similarity is satisfied by the equation (2.2.7). The variation in physical properties of a particular fluid (ρ, ν, k and c_p) with respect to temperature T is required to solve the above transformed boundary layer equations.

2.2.1   Special Cases

Case A: Constant Fluid Properties

The ODE in Eq.(2.2.8) is paired with thermal energy boundary layer Eq. (2.2.9) with respect to the temperature-dependency of density and viscosity. For constant

fluid properties, the similarity transformation variable η simplifies to:

$$\eta = \sqrt{\frac{U}{a\nu_0 x}}\, y \qquad (2.2.11)$$

which is a Blasius variable.

Therefore, Eqs. (2.2.8) and (2.2.9) reduce to

$$f'''(\eta) + \frac{a}{2} f(\eta) f''(\eta) = 0, \qquad (2.2.12)$$

and

$$\theta''(\eta) + \frac{aPr_0}{2} f(\eta)\theta'(\eta) = 0 \qquad (2.2.13)$$

These equations are still subject to the boundary conditions (2.2.10). For $a = 1$, the reduced momentum boundary layer problem is similar to that of Sakiadis [14] and Tsou et al. [21].

Case B: Variable Viscosity

Following Pop et al. [4], Andersson and Aarseth [6], Pantokratoras [20], and El-bashbeshy and Bazid [23], viscosity is considered temperature-dependent whereas other fluid properties are assumed to be constant.

For a viscous fluid, it is assumed that the viscosity is an inverse linear function of temperature given by the following equation.

$$\mu = \frac{\mu_{ref}}{[1 + \gamma(T - T_0)]} \qquad (2.2.14)$$

here γ is a fluid property that depends on the reference temperature T_{ref}. The inversely linear viscosity-temperature correlation was also used by Andersson and Aarseth [6], and Pantokratoras [20] and Elbashbeshy and Bazid [23]. If the reference temperature $T_{ref} \approx T_o$, the formula (2.2.14) can be written as follows

$$\mu = \frac{\mu_0}{1 - \frac{T-T_0}{\theta_{ref}(T_w-T_0)}} \tag{2.2.15}$$

Using above formula in Eqs. (2.2.8) and (2.2.9), we get

$$\frac{2}{a}(\frac{\mu}{\mu_0}f'')') + f(\eta)f''(\eta) = 0 \tag{2.2.16}$$

$$f''' = -\frac{a}{2}\frac{(\theta_{ref} - \theta)}{\theta_{ref}}f(\eta)f''(\eta) - \frac{f''(\eta)\theta'}{(\theta_{ref} - \theta(\eta))}, \tag{2.2.17}$$

While thermal boundary layer equation takes the same form as of Eq. (2.2.13). It should be noted that Pop et al. [4] used a transformation with $a = 1$ while Elbashbeshy and Bazid [23] chose $a = 2$.

2.3   Numerical Methods

Shooting method and *bvp4c* are used to find the numerical solution of boundary value problems. In order to solve a set of transformed differential equations with boundary conditions, we apply shooting method which is used for finding the numerical solution of the boundary value problems (BVPs). This method converts BVP into an initial value problems (IVP)by guessing the initial missing guess until the convergence is obtained.

To convert BVP into an IVP, new variables are defined as follows

$$y = f = y_1, \quad f' = y_1' = y_2, \quad f'' = y_2' = y_3$$
$$\theta = y_4, \quad \theta' = y_4' = y_5. \tag{2.3.1}$$

This method transforms the coupled ordinary differential equations (2.2.12), (2.2.13) and (2.2.16) to a system of five simultaneous equations with five unknowns. Then equations for constant fluid properties (Case A) can be written as

$$y_3' = f''' = -\frac{a}{2} y_1 y_3, \tag{2.3.2}$$

$$y_5' = \theta'' = -\frac{a Pr_0}{2} y_1 y_5. \tag{2.3.3}$$

Equation of momentum for variable fluid properties (Case B) becomes

$$y_3' = f''' = -\frac{a}{2} \frac{(\theta_{ref} - y_4)}{\theta_{ref}} y_1 y_3 - \frac{y_3 y_5}{(\theta_{ref} - y_4)}, \tag{2.3.4}$$

while thermal equation remains the same as Eq. (2.3.3).

Results obtained from shooting method are compared with the results of *bvp4c*.

2.4 Results and Discussions

The solution of boundary value problem (2.2.8) and (2.2.9) depends on T_0, Pr_0 and $T_w - T_0$. Pr_0 is related to T_0. Similar to the works of Pop et al. [4], Pantokratoras [20], and Elbashbeshy and Bazid [23] the paper of Andersson and Aarseth [6] assumes all physical properties except viscosity constant while focuses on the effects of temperature dependence of viscosity. First the numerical solution of Sakiadis problem is calculated for the constant fluid properties for $Pr_0 = 0.7$. Results of characteristic gradient velocity and temperature are compared with the results of [4], [20], [21], and [24] in Table 2.1. It serves the purpose of validating the technique

of Andersson and Aarseth [6].

Two different cases are solved to describe the effect of temperature dependent

η_∞	$-f''(0)$	$-\theta'(0)$
Sakiadis [2]	0.44375	-
Tsou et al. [21]	0.444	0.4392
Takhar et al. [7]	0.4439	0.3508
Pop et al. [4]	0.4445517	0.3507366
Pantokratoras [20]	0.4438	0.3500
8 (current)	0.4445533	0.3541256
16 (current)	0.4437512	0.3492923
24 (current)	0.4437500	0.3492374
32 (current)	0.4437507	0.3492372

Table 2.1: Numerical values of $f''(0)$ and $\theta'(0)$ for $Pr_0 = 0.7$, $a = 1$ and constant fluid properties.

viscosity. Water is considered as an ambient fluid at temperature $T_0 = 5\,°C(278K)$. Temperature of the flat surface is taken as $T_w = 85\,°C(358K)$, then $T_w - T_0 = 80K$. Results for Sakiadis problem for Case A are compared with those of Case B in Table 2.2. we have used $\theta_{ref} = -0.25$ for water at $T_0 = 278K$.

	shooting method		bvp4c	
$Case$	$-f''(0)$	$-\theta'(0)$	$-f''(0)$	$-\theta'(0)$
A	0.4437483	1.6802948	0.4437483	1.6803047
B	1.3005546	1.5291513	1.3005463	1.5291562

Table 2.2: Numerical solutions of $f''(0)$ and $\theta'(0)$ for $Pr_0 = 10$, $a = 1$.

Compared to Case A, a velocity profile $f'(\eta)$ is reduced near the surface for Case B. Viscosity reduces when surface heats the adjacent fluid. It also reduces the viscous diffusion of stream-wise momentum in the inner part of momentum boundary layer.

30

A reduced $f(\eta)$ in the advection term $(1/2a)Pr_0 f\theta'$ in thermal equation (2.2.13) causes decrease in viscosity and produces higher temperature near the surface as shown in Fig 2.2. The rise in temperature near the surface is known as an indirect effect. It should be noted that there is no direct effect of the temperature dependent viscosity in equation (2.2.13) and the importance of the diffusive energy transport θ'' is also increased [6]. Pop et al. [4] and Pantokratoras [20] did not consider the case for temperature-dependent viscosity.
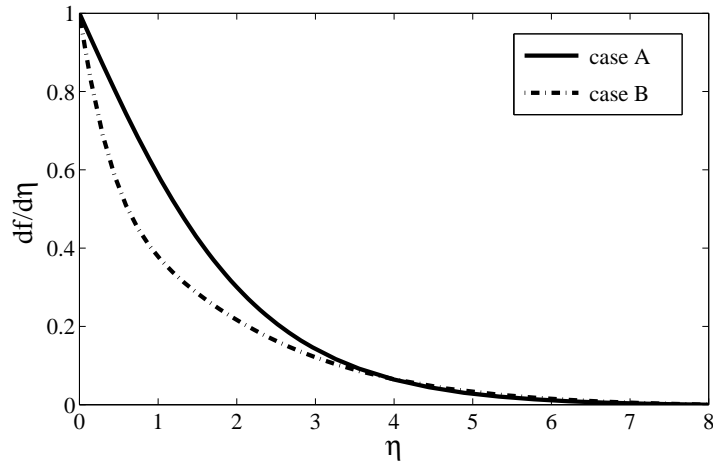
Figure 2.1: Velocity profile $f'(\eta)$ for $Pr_0 = 10$ and $a = 1$.
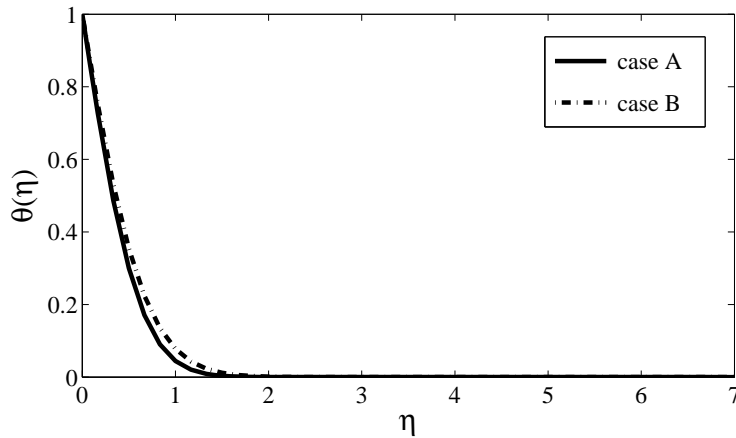
Figure 2.2: Temperature profile $\theta(\eta)$ for $Pr_0 = 10$ and $a = 1$.

The thermal gradient in Case A in Table 2.2 is accurately same as $\theta'(\eta) = -1.6804$ mentioned by Tsou et al. [21]. Andersson and Aarseth has observed a three-fold increase in the velocity gradient which shows that skin-friction appears when the temperature-dependent viscosity is considered. However, temperature gradient for Case B has been reduced by 10 percent. Though thermal boundary layer was thinner in Case A but it became thicker in Case of temperature-dependent viscosity. Since local Prandtl number Pr is less than Prandtl number of the ambient fluid Pr_0, the ratio of momentum boundary layer thickness and thermal boundary layer thickness decreases with reduced viscosity [6].

Chapter 3

Numerical Solution of Compressible Flow Over a Stretching Sheet

3.1 Introduction

The study of laminar flow over a stretching sheet in a viscous and compressible fluid is of considerable interest because of its application in the extrusion of a polymer sheet from a dye or in the drawing of plastic films. Anderson and Aarsheth [6], M. Mustafa et al. [25], M. Turkyilmazoglu [26] and M. Sheikholeslami et al. [27] revised the Sakiadis flow by considering a variable viscosity of the fluid.

An extensive work is carried out to analyse the motion of a fluid using moving and fixed surfaces. Using different flow models and boundary conditions, boundary layer flow has been observed on the stretching/continuous sheet by some authors including Anderson and Aarsheth [6], Anjalidevi and Thiyagarajn [28], Sanyal and Das Gupta [29], Takhar and Soundalgekar [30], Mahapatra et al. [31], Bhargava et al. [32], Idress and Abel [33], Takhar and Soundalgekar [34].

In this chapter, the effects of temperature-dependent physical properties are taken into account along with constant fluid properties. The variation of viscosity on temperature is taken into account to accurately predict the flow [23]. Viscosity of liquid

decreases with increase in temperature while the viscosity of gas increases with increase in temperature. However in [23], fluid was treated as incompressible. Using scaling variables, we carry out dimensionless analysis of the governing equations. Dynamic viscosity, density, and thermal conductivity exhibited power law variation with absolute temperature has been considered by Takhar et al. [24]. Despite its importance, temperature-dependent viscosity has not received much attention. This work deals both with the constant and temperature-dependent viscosity in the flow of compressible fluid over a stretching surface. To our knowledge, the present analysis seems the first attempt on the topic for compressible fluid.

3.2 Mathematical Formulation

We consider the two-dimensional laminar flow of viscous fluid driven by a continuously moving stretching sheet. Consider at $t = 0$, the sheet submerged in the fluid of density ρ and dynamic viscosity μ coincides with the plane $y = 0$. The flow is confined to $y > 0$. The sheet moves with linear velocity ax, where a is a constant. Let the temperatures T_w of sheet is kept constant. The free stream of fluid is maintained at constant T_∞. The effects of viscous dissipation are neglected. The basic equations for compressible fluid governed by the conservation for mass, momentum, and energy are as follows:

$$\frac{\partial}{\partial x}(\rho u) + \frac{\partial}{\partial y}(\rho v) = 0, \tag{3.2.1}$$

$$u\frac{\partial u}{\partial x} + v\frac{\partial u}{\partial y} = \frac{1}{\rho}\frac{\partial}{\partial y}\Big(\mu\frac{\partial u}{\partial y}\Big), \tag{3.2.2}$$

$$u\frac{\partial T}{\partial x} + v\frac{\partial T}{\partial y} = \frac{1}{\rho c_p}\frac{\partial}{\partial y}\Big(\frac{k\partial T}{\partial y}\Big), \tag{3.2.3}$$

where u and v are the velocity components along x-direction and y-direction respectively. T is the temperature inside the boundary layer, k is the thermal conductivity and c_p is the specific heat at a constant pressure. The boundary conditions on velocity and temperature are given by

34

$$u = ax, \quad v = 0, \quad T = T_w \ \text{ at } \ y = 0,$$
$$u = 0, \quad T = T_\infty \ \text{ as } \ y \to \infty. \tag{3.2.4}$$

A new similarity transformations has been developed to transform Eqs. (3.2.1), (3.2.2) and (3.2.3). The similarity transformation may be defined as a rule for combining two independent variables x and y into ODEs. We introduce the following dimensionless variables

$$\eta = \sqrt{\frac{a}{\nu_\infty}} \int \frac{\rho}{\rho_\infty} \, dy \ , \qquad \psi = \rho_\infty \sqrt{a\nu_\infty} \, x f(\eta), \tag{3.2.5}$$

$$\theta(\eta) = \frac{T - T_\infty}{T_w - T_\infty}. \tag{3.2.6}$$

Here ρ_∞ and ν_∞ are the values of ambient fluid at temperature T_∞. Here η is a similarity variable and $f(\eta)$ and $\theta(\eta)$ are new dependent variables. T_∞ is an ambient fluid temperature. It is emphasized that the transformation (3.2.6) exists only if $T_w \neq T_\infty$. The classical Sakiadis problem is obtained when the fluid viscosity becomes equal to ambient viscosity for $\theta_{ref} \to \infty$ [20]. In the special case $T_w = T_\infty$, the trivial solution $T(x, y) = T_\infty$ solves the energy Eq. (3.2.3) subject to the boundary conditions in Eq. (3.2.4).

It is important to note that θ is positive for gases and negative for liquids as mentioned in refs [4] and [22].

We define a stream function $\psi(x, y)$ by

$$\rho u = \frac{\partial \psi}{\partial y} \ , \qquad \rho v = -\frac{\partial \psi}{\partial x}. \tag{3.2.7}$$

On substituting Eqs. (3.2.5), (3.2.6), and (3.2.7) into the Eqs. (3.2.1), (3.2.2), and (3.2.3), we obtain

$$\left(\frac{\rho \mu}{\rho_\infty \mu_\infty} f''\right)' + f(\eta) f''(\eta) - f'^2 = 0. \tag{3.2.8}$$

$$\left(\frac{\rho k}{\rho_\infty k_\infty} \theta'(\eta)\right)' + Pr_\infty \theta'(\eta) f(\eta) = 0. \tag{3.2.9}$$

It should be mentioned here that in the transformed energy equation (3.2.9), the Prandtl number has been assumed constant across the boundary layer [20]. The constant Prandtl number is defined by $Pr_\infty = \mu_\infty c_p / k_\infty$.

We also transform the boundary conditions (3.2.4) into

$$f(0) = 0, \quad f'(0) = 1, \quad \theta(0) = 1 \quad \text{at} \ \ \eta = 0,$$
$$f' \to 0, \quad \theta \to 0 \quad \text{as} \ \ \eta \to \infty. \tag{3.2.10}$$

3.2.1 Special Cases

Case A: Sakiadis/Constant Fluid Properties

It should be noted that the ODE in Eq. (3.2.8) governing the flow in the momentum boundary layer is coupled to the thermal energy boundary layer Eq. (3.2.9) with respect to temperature-dependent density and viscosity. The coupling vanishes for constant fluid properties and similarity transformation variable η reduces to

$$\eta = \sqrt{\frac{a}{\nu_\infty}} \, y \tag{3.2.11}$$

36

which is a Blasius variable and related to boundary layer thickness δ by

$$\eta = \frac{y}{\delta}.$$

Where

$$\delta = \sqrt{\frac{\nu_\infty}{a}}.$$

Therefore, Eqs. (3.2.8) and (3.2.9) reduce to

$$f'''(\eta) + f(\eta)f''(\eta) - f'^2(\eta) = 0, \tag{3.2.12}$$

and

$$\theta''(\eta) + Pr_\infty f(\eta)\theta'(\eta) = 0 \tag{3.2.13}$$

The auxiliary boundary conditions are given in Eq. (3.2.10).

Case B: Temperature-dependent Viscosity

Most studies of the problems of heat transfer are based on the constant physical properties of the ambient fluid. As these properties especially viscosity may change with temperature, it is necessary to scrutinize the variation of viscosity to correctly predict the momentum and heat transfer rates.

Following Pop et al. [4], Andersson and Aarseth [6], Pantokratoras [20], and El-bashbeshy and Bazid [23] viscosity is considered temperature-dependent whereas other fluid properties are considered as constant.

It was assumed by Pop et al. [4] and followed Ling and Dybbs [35] that the viscosity is an inverse linear function of temperature for a viscous fluid and is given by the following equation

37

$$\mu = \frac{\mu_{ref}}{[1 + \gamma(T - T_\infty)]} \tag{3.2.14}$$

here γ is a fluid property and its value depends on the reference temperature T_{ref}. The inversely linear viscosity-temperature correlation was also used by Andersson and Aarseth [6], Pantokratoras [20], and Elbashbeshy and Bazid [23]. If the reference temperature $T_{ref} \approx T_\infty$, the formula (14) can be written as

$$\mu = \frac{\mu_\infty}{1 - \frac{T - T_\infty}{\theta_{ref}(T_w - T_\infty)}} \tag{3.2.15}$$

Using above formula in Eqs. (3.2.8) and (3.2.9), we get

$$\left(\frac{\mu}{\mu_\infty} f''\right)' + f(\eta) f''(\eta) - f'^2(\eta) = 0 \tag{3.2.16}$$

$$f''' = -\frac{f''(\eta)\theta'(\eta)}{(\theta_{ref} - \theta(\eta))} - \frac{(\theta_{ref} - \theta(\eta))}{\theta_{ref}}(f(\eta)f''(\eta) - f'(\eta)^2), \tag{3.2.17}$$

While thermal boundary layer equation takes the same form as of Eq. (3.2.13).

3.3 Numerical Methods

To numerically compute the set of non-linear ordinary differential equations subject to the boundary conditions, the shooting method via fifth order Runge-Kutta integration method and MATLAB built-in solver $bvp4c$ are used. To convert BVP into an IVP, we define new variables as

$$y = f = y_1, \quad f' = y_1' = y_2, \quad f'' = y_2' = y_3$$
$$\theta = y_4, \quad \theta' = y_4' = y_5. \tag{3.3.1}$$

38

This method transforms the coupled ordinary differential equations (3.2.12), (3.2.13), and (3.2.16) which are third order in f and second order in θ, to a system of five simultaneous equations with five unknowns.

Then equations for constant fluid properties (Case A) can be written as

$$y_3' = f''' = -y_1 y_3 + y_2^2, \tag{3.3.2}$$

$$y_5' = \theta'' = -Pr_\infty \, y_1 y_5. \tag{3.3.3}$$

Equation of momentum for variable fluid properties (Case B) becomes

$$y_3' = f''' = -\frac{y_3 y_5}{(\theta_{ref} - y_4)} - \frac{(\theta_{ref} - y_4)}{\theta_{ref}}(y_1 y_3 - y_2^2), \tag{3.3.4}$$

while thermal equation remains the same as Eq. (3.3.3).

3.4   Results and Discussions

The solution of the generalized boundary value problem depends on T_∞, $(T_w - T_\infty)$ and Pr_∞ as mentioned in the paper of Andersson and Aarseth [6]. Pr_∞ is related to T_∞. As in refs [6] and [20], the current work also focuses on temperature dependent viscosity while considering other fluid properties constant. Unlike other literature, the solution of equations governing variable fluid properties is also obtained in Table 3.2 for a range of values of variable η. Lai and Kulacki [22] considered a reference temperature of $80K$ for geophysical usage which gave them $\theta_{ref} = 5.62$ for air and $\theta_{ref} = -0.37$ for water but we have considered $\theta_{ref} = -0.25$ as mentioned by Andersson and Aarseth [6] and Ling and Dibb [35].

First, numerical solutions for constant and variable fluid properties are computed for Prandtl number $Pr_\infty = 0.7$ for different values of integration domain. Tsou et al. [21] numerically solved the differential equations for $Pr_\infty = 0.7, 1, 10, 100$. In Tables 3.1 and 3.2 the dimensionless velocity and temperature gradients on the sheet are estimated. The velocity boundary layer grows in the direction of motion

η_∞	$-f''(0)$	$-\theta'(0)$
8	1.00006251	0.456055378
16	1.00000004	0.453928163
24	1.00000001	0.4539168
32	1.00000003	0.453920088
40	1.00000001	0.453917639

Table 3.1: Numerical values of $f''(0)$ and $\theta'(0)$ for $Pr_\infty = 0.7$ and different values of ratio parameter η (Case A).

η_∞	$-f''(0)$	$-\theta'(0)$
8	2.28569231	0.311824842
16	2.28199354	0.291035625
24	2.28176472	0.289721023
32	2.28175165	0.289635306
40	2.28175001	0.289627223

Table 3.2: Numerical values of $f''(0)$ and $\theta'(0)$ at $Pr_\infty = 0.7$ and using variable fluid properties (Case B).

of flow. There is a very slight change in the values of velocity gradient for different domains in Tables 3.1 and 3.2 though the change is evident in different values of temperature gradient in Table 3.2. Water is taken as an ambient fluid at $T_\infty = 278K$ and $Pr_\infty = 10$ and surface temperature $T_w = 358K$. Second, results for Case A and Case B are computed in Table 3.3. We have used $\theta_{ref} = -0.25$. Also note that small values of Prandtl number (less than 1) in a given fluid indicate that thermal diffusion occurs at a greater rate than momentum diffusion. However, for Prandtl number greater than 1, momentum diffuses at the greater rate than thermal energy.

Case	$-f''(0)$			$-\theta'(0)$
	shooting method	$bvp4c$	shooting method	$bvp4c$
A	1.0000001	1.0	2.3080052	2.6781983
B	2.6784758	2.6781983	2.0388601	2.0389636

Table 3.3: Numerical values of $f''(0)$ and $\theta'(0)$ and $Pr_\infty = 10$.
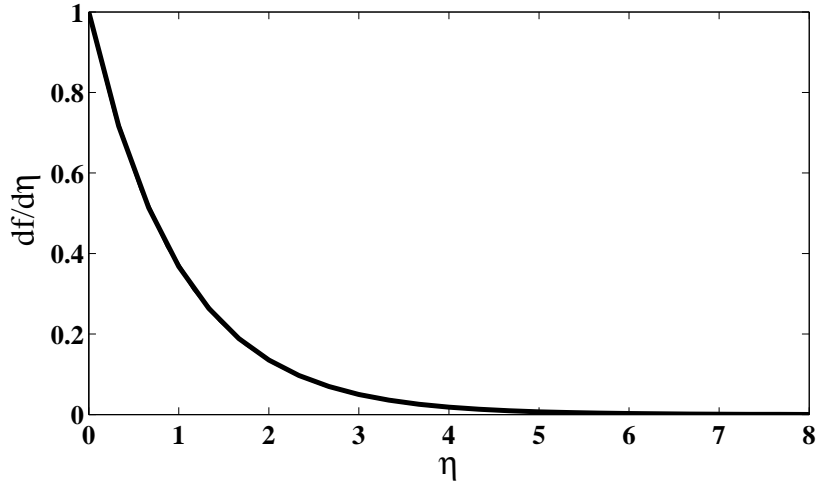
Figure 3.1: (Case A) Velocity profile $f'(\eta)$ for $Pr_\infty = 0.7$.

The computed velocity $f'(\eta)$ and temperature profiles $\theta(\eta)$ are shown in Figs. 3.2-3.7, respectively. Figs. 3.2 and 3.3 are drawn for constant fluid properties while Figs. 3.4 and 3.5 are displayed for variable fluid properties (Case B) when considering a range of values of η in both cases. There is a very slight change in the values of velocity profile in the Figs 3.2 and 3.4. Similarly, there is hardly any effect in the temperature gradient $\theta(\eta)$ for different values of η in Figs. 3.3 and 3.5. There are only marginal differences in the surface gradients between Case A and Case B for different values of η and $Pr_\infty = 0.7$. The thermal boundary layer is slightly thicker than the momentum boundary layer when considering $Pr_\infty = 0.7$. Velocity profile
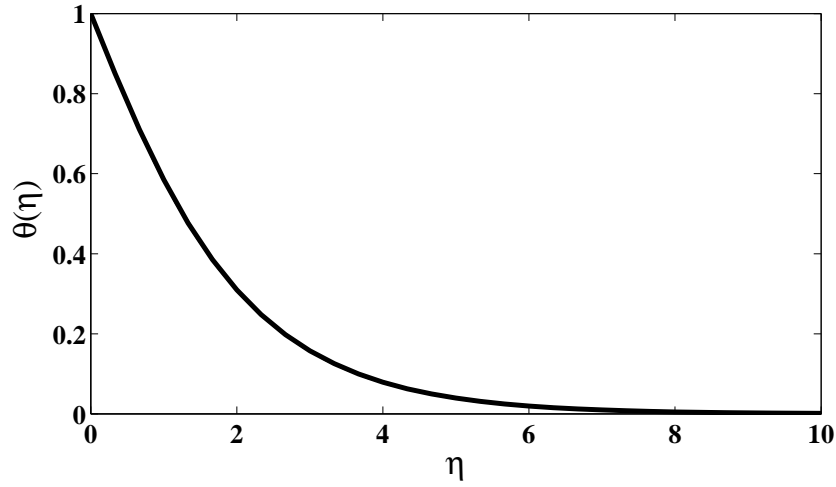
Figure 3.2: (Case A) Temperature profile $\theta(\eta)$ for $Pr_\infty = 0.7$.

$f'(\eta)$ in Fig. 3.6 is substantially reduced near the moving surface for Case B when compared with Case A. Also boundary layer thickness is reduced for Case B. The momentum layer thickness at zero velocity has the same momentum defect relative to the outer flow as the actual boundary layer [15]. Approximately twofold increase in the velocity gradient at the stretching sheet is observed when Case B is taken into account. An 11 percent reduction in temperature gradient is observed for Case B when compared to Case A. The temperature profiles θ in Fig. 3.7 show higher temperature near the surface due to the reduced viscosity. The thermal boundary layer becomes slightly thicker in Case B where temperature-dependent viscosity is considered. Note that thermal boundary layer develops when the stretching sheet's temperature T_w is different from free-stream temperature T_∞. There is an indirect effect of the temperature dependent viscosity on the governing thermal equation (3.2.13).

Figure 3.3: (Case B) Velocity profile $f'(\eta)$ for $Pr_\infty = 0.7$.
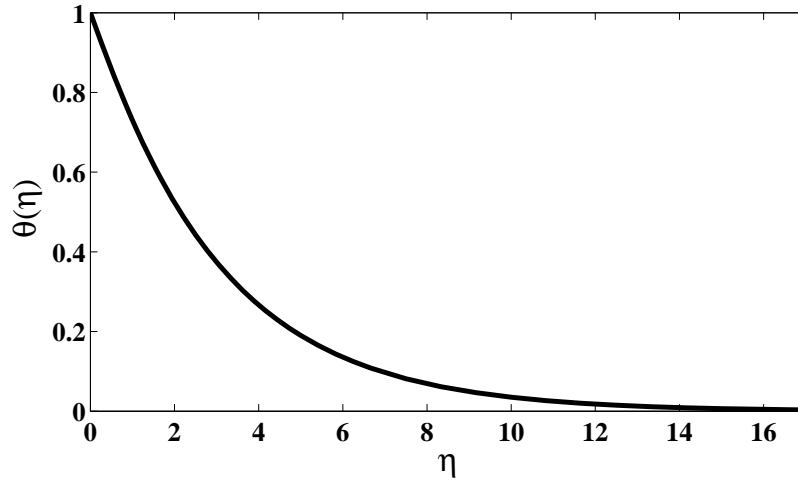
Figure 3.4: (Case B) Temperature profile $\theta(\eta)$ for $Pr_\infty = 0.7$.

3.4.1 Prandtl Number and Integration Domain

Due to difference in temperatures of the surface and ambient fluid, convection appears. A large number of parameters can be involved in solving conservation equa-
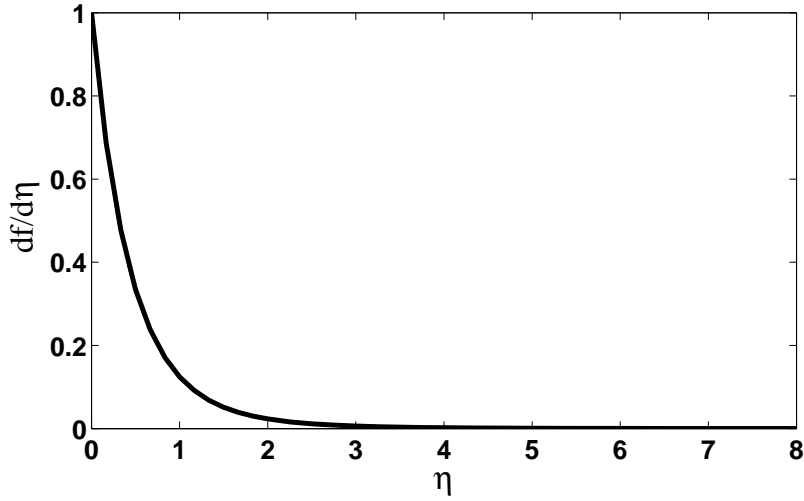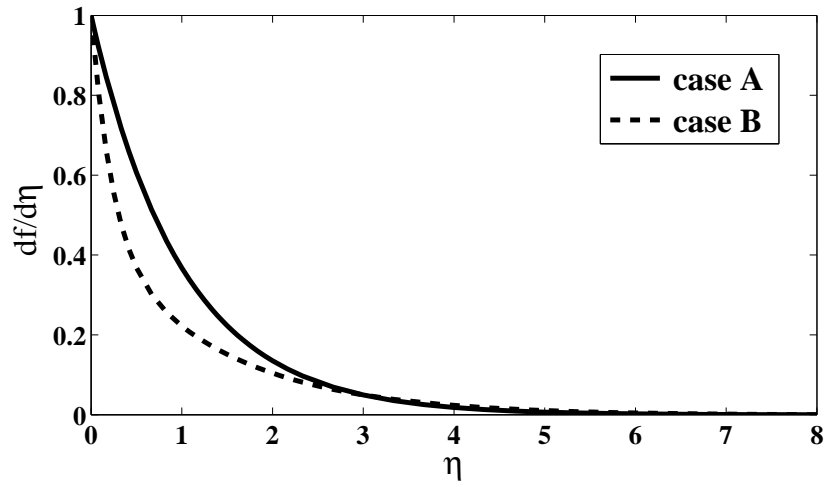
Figure 3.5: Velocity profile $f'(\eta)$ for $Pr_\infty = 10$.
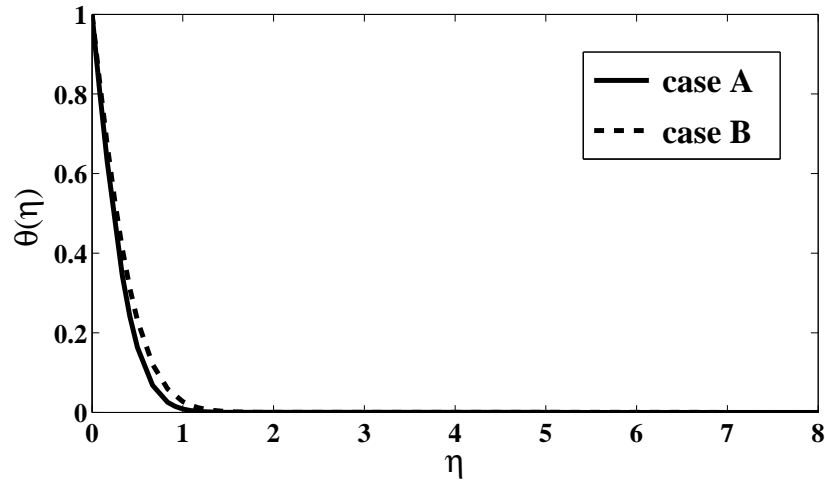
Figure 3.6: Temperature profile $\theta(\eta)$ for $Pr_\infty = 10$.

tions for convection. The heat transfer coefficient is usually expressed using a non-dimensional group that also includes Prandtl number. The Prandtl number appears

44

in both natural and free convection. The Prandtl number is the ratio of the rate when viscous forces penetrates the material to the rate when thermal forces penetrates the material. As a consequence, Prandtl number is proportional to the rate of growth of two boundary layers, i.e.

$$\frac{\delta}{\delta_T} \approx Pr^{1/2}. \tag{3.4.1}$$

This suggests that δ/δ_T should decrease due to the reduced viscosity [6].
The physical properties of fluid depends upon temperature, so the Prandtl number $Pr = \mu c_p/k$ also varies with temperature. Pantokratoras [20] used the Prandtl number that varied with viscosity. Takhar et al. [24] also considered variable Prandtl number. However in the present work, the constant Prandtl number Pr_o of ambient fluid is used into the transformed equations (3.2.8)-(3.2.10) which also appeared in the works of Pop et al. [4] and Elbashbeshy and Bazid [23]. Moreover, Takhar et al [24] used gases while Andersson and Aarseth [6] has considered water. For gases Prandtl number may be considered constant in the temperature range of T_w and T_∞ while for liquids, its temperature variation may be essential. It is noted that Prandtl number of water decreases with increase in temperature which is due to the reduction in μ and increase of 20% in thermal conductivity k.
Pantokratoras [20] solved the BVP on a finite-interval $\eta \in [-10, 10]$ without using similarity transformation. He used $Pr_\infty = 0.7$ and 10. Pop et al. [4] integrated the resulting BVP over the interval $\eta \in [0, 8]$ for $Pr_\infty = 0.7$ and $\eta \in [0, 4]$ for $Pr_\infty = 10$. The results in their papers show that interval domain is not large enough for the proper decay of velocity and temperature profiles. Thus the auxiliary result

$$f'' \to 0; \quad \theta' \to 0 \ as \ \eta \to \infty \tag{3.4.2}$$

is violated. However, the non-linear BVP (3.2.8)-(3.2.10) are defined on the infinite interval $\eta \in [-\infty, \infty]$ in order to satisfy the outer boundary conditions in (3.2.10) and auxiliary condition (3.4.2).

Chapter 4

Numerical Solution of Compressible Euler Equations

4.1   Introduction

In this chapter, we numerically solve compressible Euler equations in one dimension. For time integration, we use Euler method and for space discretization, we apply Lax-Friedrichs methods. For test case, 1D shock tube problem is solved.

4.2   Governing Equation

A nonlinear hyperbolic conservation law in one dimension takes the form

$$\frac{\partial U}{\partial t} + \frac{\partial F(U)}{\partial x} = 0. \tag{4.2.1}$$

Here F is the flux vector which usually arises from the transport of conservative variable U in the domain. As conservation law consists of equations of mass, momentum and energy, therefore, U and F in vector form are defined as

$$U = \begin{bmatrix} \rho \\ \rho u \\ \rho E \end{bmatrix} \qquad (4.2.2)$$

It represents mass per unit volume, momentum per unit volume and total energy per unit volume, respectively. The flux is given by

$$F = \begin{bmatrix} \rho u \\ \rho u^2 + p \\ u(\rho E + p) \end{bmatrix} \qquad (4.2.3)$$

Conservation law comprises of equations of mass, momentum, and energy. There are three equations and four unknowns which are density, velocity, pressure and total energy. To find a solution, we require an equal number of equations and unknowns. Here we introduce one more equation known as equation of state that determines the nature and type of fluid. Equation of state is form of conservation on a microscopic level [37]. For perfect gas, pressure p, density ρ, and temperature T are related by the thermal equation of state

$$p = \rho R T, \qquad (4.2.4)$$

which is a conservation of momentum on the microscopic level. Similarly a relation between an internal energy e and constant volume specific heat c_v expressed by caloric equation of state is in fact a conservation of energy on the microscopic level, which is

$$e = c_v T, \qquad (4.2.5)$$

where

$$R = c_p - c_v$$

is a specific gas constant. c_p is constant pressure specific heat. For air at standard sea-level, $c_p = \frac{\gamma R}{\gamma - 1} = 1004.5 m^2/s^2 k$ and $c_v = \frac{R}{\gamma - 1} = 717.5 m^2/s^2 k$. Also $e = e(T)$ for thermal equation of state. Note that a fluid obeying the thermal equation of state is

47

called thermally perfect while one following caloric equation of state is called calorically perfect. And gas obeying both laws is called a perfect gas.

Solving equations (4.2.4) and (4.2.5) give

$$p = \rho e (\gamma - 1) \tag{4.2.6}$$

here $\gamma = \frac{c_p}{c_v}$ is the ratio of specific heats, calls adiabatic exponent. For air at standard condition, $\gamma = 1.4$, $R = 277 m^2/s^2 k$. The total energy E is often defined as

$$E = e + \frac{1}{2} u^2 \tag{4.2.7}$$

e is the internal energy and $u^2/2$ is the kinetic energy. Equation (4.2.4) can also be written as

$$p = (\gamma - 1)(\rho E - \frac{1}{2} \rho u^2) \tag{4.2.8}$$

4.3 Characteristic Equation

Considering a compressible Euler equation (4.2.1) in conserved and non-conserved form

$$\frac{\partial U}{\partial t} + \frac{\partial F(U)}{\partial x} = 0,$$
$$\frac{\partial U}{\partial t} + A \frac{\partial U}{\partial x} = 0. \tag{4.3.1}$$

Where $A(U) = \frac{dF}{dU}$ is a Jacobian matrix. The equation (4.3.1) is a quasi-linear nonconservative hyperbolic equation. This equation is hyperbolic if and only if A has real eigenvalues and is diagonalizable, i.e. $R^{-1}AR = \Lambda$ for some matrix R [37]. Λ is a diagonal matrix.

Multiplying both sides of equation (4.3.1) by R^{-1}, we obtain.

$$R^{-1}\frac{\partial U}{\partial t} + R^{-1}A\frac{\partial U}{\partial x} = 0. \tag{4.3.2}$$

48

By changing the characteristic variable $V = R^{-1}U$, above equation becomes

$$\frac{\partial V}{\partial t} + \Lambda \frac{\partial V}{\partial x} = 0, \tag{4.3.3}$$

which is a characteristic form of equation (4.3.1) that is written in characteristic variable V. It is in fact a wave-form. Equation (4.3.1) can also be written in form of V as

$$V_i = constant, \quad for \quad \frac{dx}{dt} = \lambda_i. \tag{4.3.4}$$

V_i are signals carried by waves, $dx = \lambda_i \, dt$ are called wavefronts or characteristic curves, and λ_i are wave speeds or characteristic speeds [37].

A matrix A for conservative form of compressible Euler equation is given by

$$A = \begin{bmatrix} 0 & 1 & 0 \\ (\gamma - 3)u^2/2 & (3 - \gamma)u & \gamma - 1 \\ -\gamma eu + (\gamma - 1)u^3 & \gamma e - 3(\gamma - 1)u^2/2 & \gamma u \end{bmatrix} \tag{4.3.5}$$

The eigenvalues of A obtained by $det(\lambda I - A)$ are

$$\lambda_1 = u, \quad \lambda_2 = (u + a), \quad and \quad \lambda_3 = (u - a) \tag{4.3.6}$$

Since $R^{-1}AR = \Lambda$, where matrices R^{-1} and R are left and right characteristic vectors of A, respectively. To find right characteristic vectors of A associated with λ_i, $i = 1, 2, 3$, we define $(\lambda_i I - A)r$ and to find left characteristic vectors of A, we define $(\lambda_i I - A)l$. Where I is an identity matrix, r are a right characteristic vectors and l are left characteristic vectors.

As $R = [r_{A_1} | r_{A_2} | r_{A_3}]$ and $R^{-1} = [l_{A_1} | l_{A_2} | l_{A_3}]$, we get

$$R = \begin{bmatrix} 1 & \frac{\rho}{2a} & -\frac{\rho}{2a} \\ u & \frac{\rho}{2a}(u + a) & -\frac{\rho}{2a}(u - a) \\ \frac{u^2}{2} & \frac{\rho}{2a}\left(\frac{u^2}{2} + \frac{a^2}{\gamma-1} + au\right) & -\frac{\rho}{2a}\left(\frac{u^2}{2} + \frac{a^2}{\gamma-1} - au\right) \end{bmatrix} \tag{4.3.7}$$

49

and

$$R^{-1} = \frac{\gamma - 1}{\rho a} \begin{bmatrix} \frac{\rho}{a}(-\frac{u^2}{2} + \frac{a^2}{\gamma-1}) & \frac{\rho}{a}u & -\frac{\rho}{a}u \\ \frac{u^2}{2} - \frac{au}{\gamma-1} & -u + \frac{a}{\gamma-1} & 1 \\ -\frac{u^2}{2} - \frac{au}{\gamma-1} & u + \frac{a}{\gamma-1} & -1 \end{bmatrix} \tag{4.3.8}$$

There is a physical relation between the flow and characteristics. The wave speed λ_1 equals to flow speed u while the wavefronts $dx = \lambda_1 \, dt = u \, dt$ is equal to pathlines. Thus first family of waves travels with the fluid and is called entropy (contact discontinuity)wave. In case of remaining two family of characteristics, $dx = (u+a) \, dt$ conforms to travel at the local speed of flow in addition to local speed of sound, whereas $dx = (u-a) \, dt$ conforms to travel at the local speed of flow minus the local speed of sound. Later two families of characteristics are called acoustic waves.

4.4 Numerical Methods

Different finite difference methods are used to solve compressible Euler equation. One of them is Lax Friedrich Method (LFM). LFM is an explicit, consistent, and conservative method. It is based on Forward-Time Centre-Space method which can be written as

$$U_i^{n+1} = U_i^n - (\Delta t/2\Delta x)(F_{i+1}^n - F_{i-1}^n). \tag{4.4.1}$$

Here numerical flux can be defined as

$$F(U_{i+1}^n, U_i^n) = \frac{1}{2}(F(U_{i+1}^n) + F(U_i^n)) - \frac{\Delta x}{2\Delta t}(U_{i+1}^n - U_i^n). \tag{4.4.2}$$

The flux is a centered flux. The additional term $\frac{\Delta t}{\Delta x}$ is called numerical diffusion or viscosity and LFM introduces too much diffusion. LFM can be improved by replacing numerical viscosity by $\max(abs(F'(u_l), F'(u_r)))$. This method is called Rusanov's method or local Lax-Friedrich Method. Lax-Friedrich Method converges to the true solution as $\Delta x \to 0$ and $\Delta t \to 0$, provided CFL is satisfied. LFM is first order accurate in space and time.

CFL of Lax Friedrich can be defined as

$$CFL = \max(abs(u + a))\Delta t/\Delta x \le 1. \tag{4.4.3}$$

4.5 Test Case: Shock Tube Problem

We are studying a shock tube in gas-dynamics. A simple shock tube is an instrument which is used to study blast wave effects under laboratory conditions. It is a long tube or cylinder divided into two chambers by diaphragm. It has a constant area.
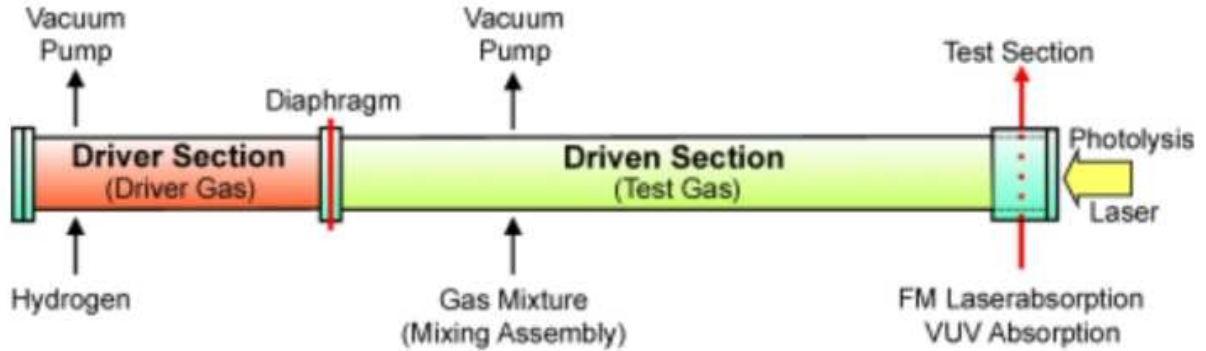

Figure 4.1: Diagram of shock tube [41].

The chamber consisting of high pressure gas is called driver chamber while chamber containing low pressure gas is called driven or expansion chamber. These regions can consist of different gases that are at rest. Let their ratio of specific heats is denoted by γ_1 and γ_2, respectively. Also the data at initial stage is T_1, p_1, u_1, ρ_1 on the right side of the tube and T_2, p_2, u_2, ρ_2 on the left side. When diaphragm is ruptured at time $t = 0$, the gas from the high pressure chamber flows into the low pressure chamber and compresses it. It causes an unsteady flow containing steadily moving shock wave, expansion wave and contact wave. A normal shock wave propagates into low pressure region and expansion wave propagates into high pressure region [37]. A temperature reaches in thousand of degrees within a short interval.

A gas of low molecular weight like helium or hydrogen is chosen for driver region. In fact the molecular weights μ_1 and μ_2 of both gases are different. The driver and driven gases don't coalesce due to the presence of contact surface in the driven chamber. Pressure and velocity are same across that surface. Shock wave and expansion or rarefaction wave reflect at the closed ends of tube. The reflected shock wave cancels the motion of the driven gas that is caused by the primary shock. A
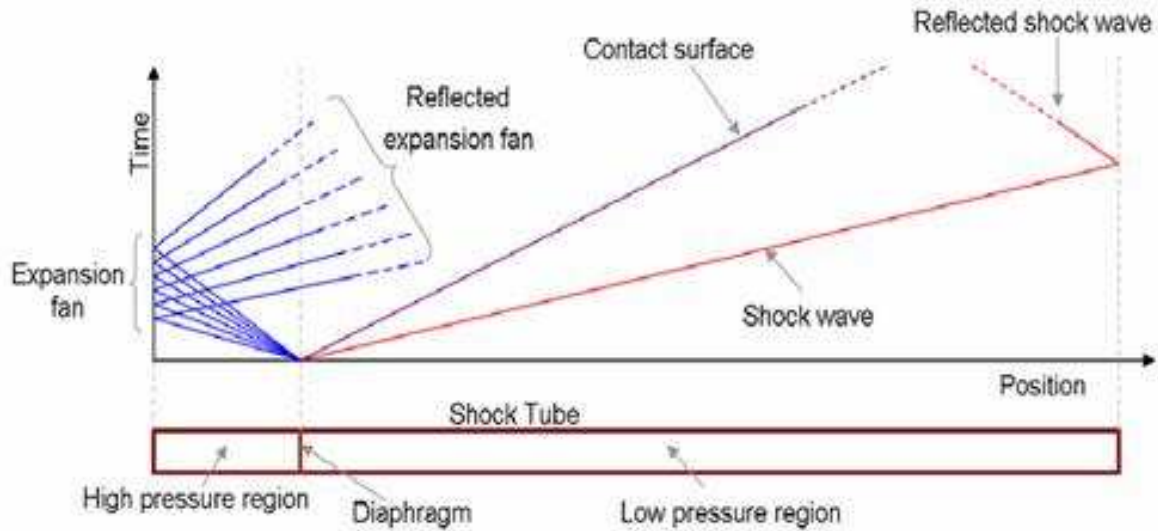
Figure 4.2: Shock and expansion waves produced in a shock tube [38].

shock wave originate either from jump-discontinuity in the initial condition or from smooth compression wave. Mach number increases as the pressure ratio across diaphragm increases.

Expansion or rarefaction waves are always composed of acoustic waves whereas entropy waves don't produce expansion waves [37]. In other words, expansion waves are created by family of characteristics containing $u + a$ and $u - a$. Unlike shock, expansion waves are composed of boundaries. The boundary at high pressure side is called head and at low pressure side is called tail of expansion. An expansion wave appears like an old fashioned fan, so it is also called expansion fan. All characteristics originate from a single point in the $x - t$ plane in the centered expansion fan. That single point can be either a jump discontinuity in the initial conditions or an intersection between shocks or contact discontinuities [37]. The flow across expansion can be solved using method of characteristics.

Contact discontinuity like shocks is a jump continuity. It can't form immediately and originate either in the initial condition or at the intersection of the shocks. It flows with the fluid but fluid doesn't pass through contact discontinuity. Also note that pressure and velocity are equal across contact but density and energy are dif-

ferent.

4.6 Riemann Problem for Compressible Euler Equation

Shock tube problem gives rise to shock, expansion and contact waves but in case of Riemann problem, one or two of these waves may be absent. Unlike the integral form, the differential form of compressible Euler equations contain undifferentiated discontinuities that create shock waves. The non-differentiable solution is called a weak solution. Riemann problem finds the weak solution of the equation. The initial condition of Riemann problem for compressible Euler equation at $x = x_o$ and $t = t_o$ is

$$u\,(x, t_o) = \begin{cases} u_l & \text{for } x < x_o \\ u_r & \text{for } x > x_o \end{cases} \tag{4.6.1}$$

The Riemann problem is treated on an infinite domain . Unlike shock tube, the initial velocity of Riemman problem may not be zero. Here we are interested in $x_o = 0$ and $t_o = 0$ when $u_l = u_r = 0$ at the initial stage and $p_l > p_r$ and $\rho_l > \rho_r$. The driver gas is filled in the driver chamber at $x < 0$ while driven gas is filled in the driven chamber at $x > 0$.

To find a jump-discontinuities in the differential form of compressible Euler equation, Rankine-Hugoniot relations are used. We choose a rectangular control-volume that is surrounding the discontinuity and separating the left and right state of the shock. Let shock is moving in a very short time increment, say, from t_1 to $t_1 + \Delta t$ and from x_1 to $x_1 + \Delta x$. Applying an integral form of conservation law,

$$\int_{x_1}^{x_1+\Delta x} u(x, t_1+\Delta t)\,dx - \int_{x_1}^{x_1+\Delta x} u(x, t_1)\,dx = \int_{t_1}^{t_1+\Delta t} f(u(x_1, t))\,dt - \int_{t_1}^{t_1+\Delta t} f(u(x_1+\Delta x, t))\,dt,$$

since u is constant along edge, it becomes

$$\Delta x\,(u_r - u_l) = \Delta t(f(u_l) - f(u_r)).$$

53

If S is a shock speed, then $\Delta x = -S\Delta t$ when $S < 0$. Dividing by $-\Delta t$ and taking $\Delta t \to 0$, Rankine-Hugoniot equation becomes

$$S(u_r - u_l) = f_r - f_l. \tag{4.6.2}$$

Shock wave is governed by R-H relation and also satisfies the conditions of compression which is

$$u_l + a_l \geq S \geq u_r + a_r \tag{4.6.3}$$
$$\text{or} \quad u_l - a_l \geq S \geq u_r - a_r.$$

4.7 Results

For a numerical solution, the flow is assumed to be unsteady and one-dimensional. At $t = 0$, the values of flow properties $\rho_l = 1$, $p_l = 2.5$, $u_l = 0$, and $\rho_r = 0.125$, $p_r = 0.25$, $u_r = 0$ are considered on both sides of shock tube. For diatomic gas, $\gamma = 1.4$ is taken. The compressible Euler equation is solved along the initial conditions on the region $[-1, 2]$. As different numerical methods use slightly different CFL number, an initial Courant number $C = 0.34$ is chosen in the present work. Graphs are plotted for the unknown variables density, velocity, pressure and total energy. It is observed that at $\lambda_1 = u$, there is neither shock nor rarefaction wave. Instead we obtain contact discontinuities that propagate with speed equal to the characteristic speed u. Moreover, u and p are constant here and only ρ varies.

The solution of Riemann problem consists of flat regions for first order method while for second and higher order methods it develops large spurious oscillations. There is a jump in density across the contact discontinuity in the Figure 4.4. The velocity remains the same on both side of contact discontinuity and fluid never cross this path as shown in Figure 4.5. Note that the fluid is accelerated smoothly through the rarefaction wave and abruptly through the shock. Also gas in left chamber is cooled by expansion (or rarefaction) wave while gas in the right chamber heats up because of shock wave.

For initial velocity $u_l = u_r = 0$, Riemann solution consists of one shock wave and one expansion wave along a contact discontinuity. However for nonzero initial velocities, solution may consist of two shock or two expansion waves depending on the data [40].
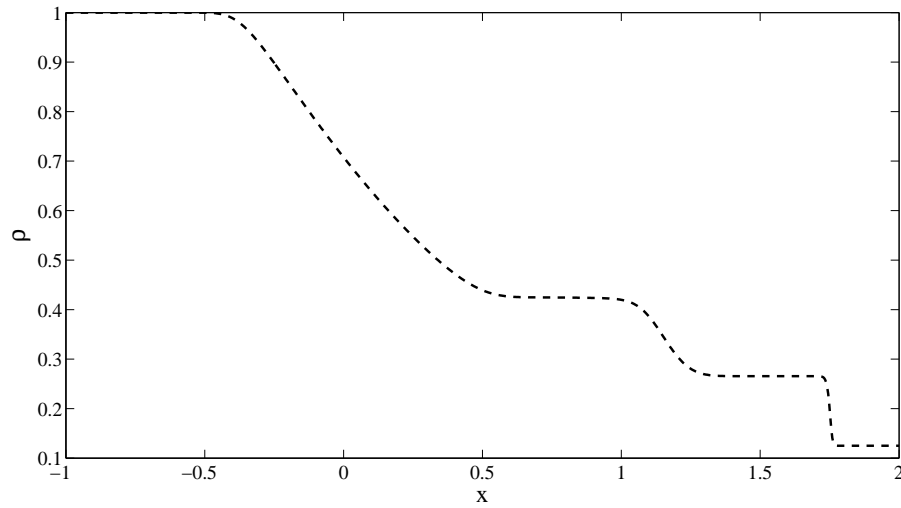

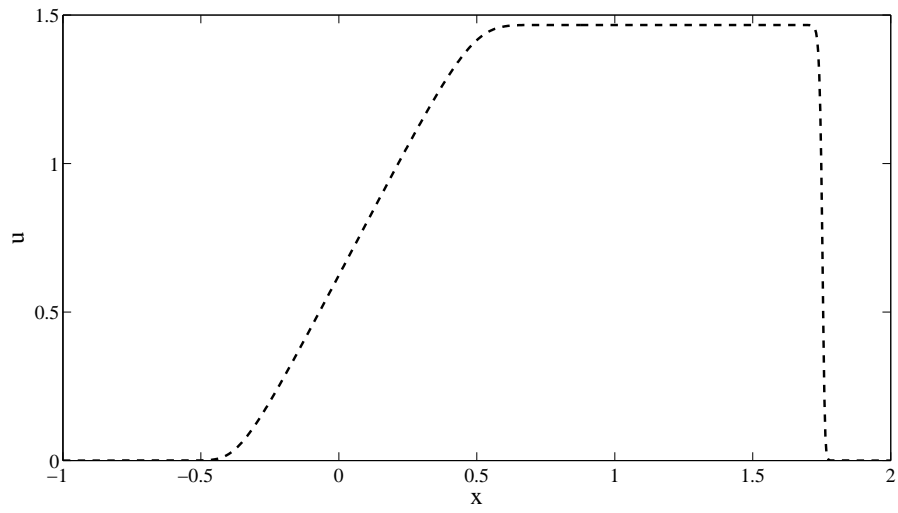Figure 4.3: Density in shock tube problem using LFM.

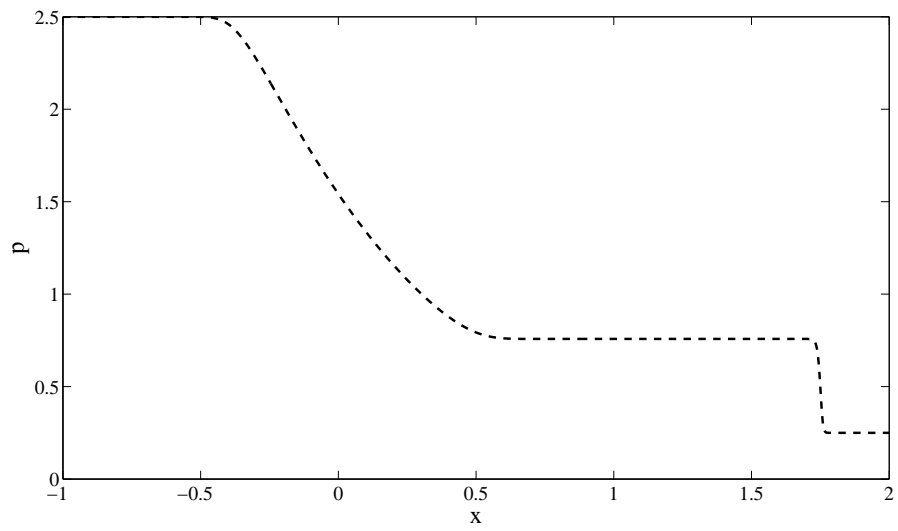Figure 4.4: Velocity in shock tube problem using LFM.

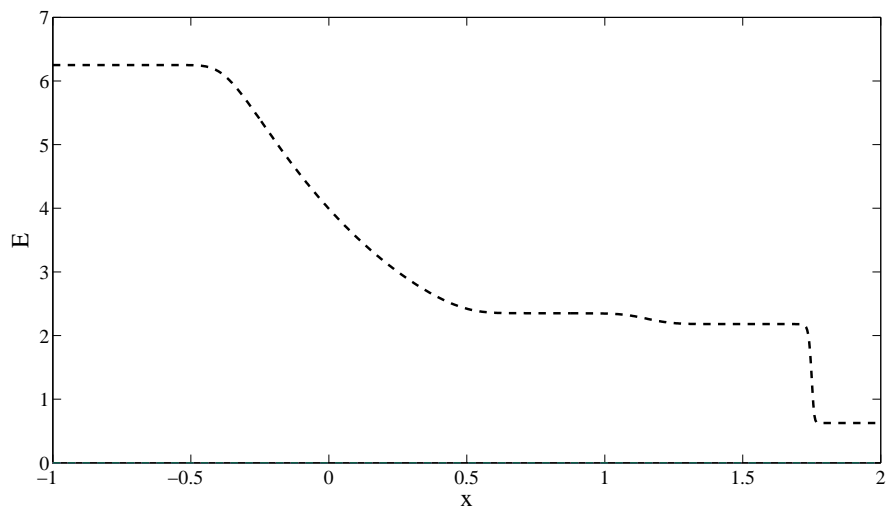Figure 4.5: Pressure in shock tube problem using LFM.

56

Figure 4.6: Total energy in shock tube problem using LFM.

Chapter 5

Conclusion and Outlook

Numerical solutions of compressible fluid were studied in two different situations.
In the first part of this thesis, we observe the effects of variable viscosity and Sakiadis
problem is studied. A laminar boundary layer behaviour of compressible fluid has
been investigated on a continuous flat surface and linearly stretching sheet. Similar-
ity transformations are applied to transform non-linear partial differential equations
(PDEs) into ordinary differential equations (ODEs). Here the dependency of vis-
cosity was considered on temperature when pressure decreases with the increase in
temperature.

Numerical methods are applied on the resultant ODEs. For that *bvp4c* and shooting
method are used. Results are plotted for Cases A and B. For temperature gradient
in Case B, a less than 10% reduction is observed for continuously moving flat surface
while approximately 11% reduction is calculated for stretching sheet. Similarly for
velocity gradient in Case B, three-fold increase is obtained for continuously moving
flat surface whereas two-fold increased is observed for stretching sheet.

The test case of shock tube problem is used in the second part of the study of the
compressible flow. A nonlinear compressible Euler equation has been derived from
a first-order non-linear hyperbolic differential equations. For time integration, an
explicit Euler method is used while for spatial integration, Lax-Friedrich and local
Lax-Friedrich Methods are used. The graphs of density, velocity, pressure, and total
energy are plotted and studied for shock and expansion waves.

Bibliography

[1] B. C. Sakiadis, *Boundary-layer behaviour on continuous solid surfaces: I. boundary-layer equations for two-dimensional and axisymmetric flow*, American International Chemical Engineers Journal, (1961), pp 26–28.

[2] B. C. Sakiadis, *Boundary-layer behaviour on continuous solid surfaces: II. The boundary-layer flow on a continuous flat surface*, American International Chemical Engineers Journal, (1961), pp 221–225.

[3] H. Blasius, *Grenzschichten in flussigkeiten mit kleiner reibung*, Z Angew Math Physics, (1908), pp 1–37.

[4] Ioan Pop, Rama Subba Reddy Gorla, and Majid Rashidi, *The effect of variable viscosity on flow and heat transfer to a continuous moving flat plate*, International Journal of Engineering and Sciences, Volume 30, (1992), pp 1-6.

[5] Junaid Ahmad Khan, M. Mustafa, T. Hayat, and A. Alsaedi, *Three-dimensional flow of nanofluid over a non-linearly stretching sheet: An application to solar energy*, International Journal of Heat and Mass Transfer, Volume 86, (2015), pp 158–164.

[6] Helge Andersson and Jan Aarseth, *Sakiadis flow with variable fluid properties revisited*, International Journal of Engineering and Sciences, Volume 45, (2007), pp 554-561.

[7] H.S. Takhar , S. Nitu, and I. Pop, *Boundary layer flow due to a moving plate: variable fluid properties*, Acta Mechanica, Volume 90, (1991), pp 37-42.

[8] John Cimbala and Yunus A. Çengel, *Fluid mechanics: fundamentals and applications*, The McGraw-Hill Companies, 1st edition, (2006).

[9] Adrian Bejan and Allan D. Kraus, *Heat transfer handbook*, Wiley-Interscience, (2003).

[10] C. P. Kothandaraman, *Fundamentals of heat and mass transfer*, New Age International Limited, 3rd edition, (2006).

[11] John Mwaonanji, *Boundary layer flow over a flat moving surface with temperature dependent viscosity*, M.Phil. thesis, University of Dar-es-Salaam,(2012).

[12] Pijush. K. Kundu, Ira M. Cohen, and Daivd R. Dowling, *Fluid mechanics*, Academic Press, 5th edition, (2012).

[13] Buddhi N. Hewakandamby, *A first course in fluid mechanics for engineers*, bookboon, 1st edition, (2012).

[14] H. Versteeg and W. Malasekra, *An introduction to computational fluid dynamics*, Prentice Hall, 2nd edition, (2007).

[15] I. G. Currie, *Fundamental mechanics of fluids*, Marcel Dekker, 3rd edition, (2003).

[16] John D. Anderson,Jr., *Computational fluid dynamics: The basics with application*, McGraw-Hill, 1st edition, (1995).

[17] A. R. Paterson, *A first course in fluid dynamics*, Cambridge University Press, 1st edition, (1984).

[18] Lokenath Debnath, *Nonlinear partial differential equations for scientists and engineers*, Springer Science, 3rd edition, (1984).

[19] Professor D. M. Causon, Professor C. G. Mingham and Dr. L. Qian, *Introductory finite volume methods for PDEs*, bookboon.com, 1st edition, (2011).

[20] A. Pantokratoras, *Further results on the variable viscosity on flow and heat transfer to a continuous moving flat plate*, International Journal of Engineering and Sciences, Volume 42, (2004), pp 1891-1896.

[21] F. K. Tsou, E. M. Sparrow, and R. J. Goldstein, *Flow and heat transfer in the boundary layer on a continuous moving surface*, International Journal of Heat and Mass Transfer, Volume 10, (1967), pp 219–235.

[22] F. C. Lai and F. A. Kulacki,*The effect of variable viscosity on convective heat transfer along a vertical surface in a saturated porous medium,*International Journal of Heat and Mass Transfer, Volume 33, (1990), pp 1028-1031.

[23] E. M. A Elbashbeshay, and M. A. A. Bazid, *The effect of temperature-dependent viscosity on heat transfer over a continuous moving surface*, Journal Physics D: Applied Physics,(2000), pp 2716–2721.

[24] H.S. Takhar , S. Nitu, and I. Pop, *Boundary layer flow due to a moving plate: variable fluid properties*, Acta Mechanica, Volume 90, (1991), pp 37-42.

[25] Junaid Ahmad Khan, M. Mustafa, T. Hayat, and A. Alsaedi, *Three-dimensional flow of nanofluid over a non-linearly stretching sheet: An application to solar energy*, International Journal of Heat and Mass Transfer, Volume 86, (2015), pp 158–164.

[26] M. Turkyilmazoglu, *Bdewadt flow and heat transfer over a stretching stationary disk*, International Journal of Mechanical Sciences, Volume 90, (2015), pp 246-250.

[27] M. Sheikholeslami, Davood D. Ganji, M. Younus Javed, and R. Ellahi, *Effect of thermal radiation on magnetohydrodynamics nanofluid flow and heat transfer by means of two phase model*, International Journal of Magnetism and Magnetic Materials, Volume 374, (2015), pp 36-43.

[28] , S. P. Anjalidevi and M. Thiyarajan, *Non-linear hydro-magnetic flow and heat transfer over a surface stretching with power law velocity*, Journal of Heat and Mass transfer, Volume 38, (2002), pp 407-413.

[29] D. C. Sanyal and Das Gupta, *Stead flow and heat transfer of a conducting fluid caused by stretching porous wall*, Indian Journal Theoretical Physics, Volume 51, (2003), pp 47-58.

[30] V. M. Soundalgekar, H.S. Takhar, V. N. Das, R. R. Deka, and A. Sarmah, *Effect of variable viscosity on a boundary layer flow along a continuous moving plate with variable surface temperature*, Journal of Heat and Mass transfer, Volume 40, (2004), pp 421-424.

[31] T. R. Mahapatra and A. S. Gupta, *Heat transfer in a stagnation point flow towards stretching sheet*, Journal of Heat and Mass transfer, Volume 38, (2002), pp 517-521.

[32] Bhargava R Kumar and H. S. Takhar, *Mixed convection from a continuous surface in a parallel moving stream of micro-polar fluid*, Journal of Heat and Mass transfer, Volume 39, (2003), pp 407-413.

[33] M. K. Idress and M. S. Abel, *Visco-elastic flow past a stretching sheet in a porous medium and heat transfer with internal heat source*, Indian journal Theoretical Physics, Volume 44 (1996), pp 233-244.

[34] H.S. Takhar and V. M. Soundalgekar, *Flow and heat transfer of micro-polar fluid past of a continuous moving porous plate*, International journal of engineering science, Volume 23, (1985), pp 201-209.

[35] J. X Ling and A. Dybbs, *Forced convection over a flat plate submersed in a porous medium:variable viscosity case*, American Society of Mechanical Engineers, Volume 114, (1987), pp 87-WA/HT-23.

[36] Lawrence F. Shampine, Jacek Kierzenka and Mark W. Reichelt, *Solving boundary value problems for ordinary differential equations in matlab with bvp4c*, CEM-UVM, (2000).

[37] Culbert B. Laney, *Computational gasdynamics*, Cambridge University Press, (1998).

[38] Genick BarMeir, *Fundamentals of compressible fluid mechanics*, (2009).

[39] Ian H. Hutchinson and Massachusetts Institute of Technology, *Two point boundary conditions*, Plasma Science and Fusion Centre, (2014), http://silas.psfc.mit.edu/22.15/lectures/chap3.xml.

[40] Randall J. LeVeque, *Finite volume methods for hyperbolic problems*, Cambridge University Press, (2004).

[41] Mechanical Engineering and University of Mississippi, *Blast and impact dynamic lab*, http://www.engineering.olemiss.edu/mechanical/facilities/blast.html.

[42] Engineering Toolbox, *Water thermal properites*, http://www.engineeringtoolbox.com/water-thermal-properties.html.

Appendix A

Tables

Temperature (C)	Prandtl number (Pr)
0.01	13.67
10	9.47
20	7.01
30	5.43
40	4.34
50	3.56
60	2.99
100	1.75
140	1.25
200	0.92

Table 5.1: Prandtl number of water at different temperatures [42].

Temperature (C)	Prandtl number (Pr)
-73	0.736
27	0.707
52	0.701
102	0.692
127	0.688

Table 5.2: Prandtl number of dry air at different temperatures [42].

Gas	Specific heats		Ratio of Specific heats	Gas constant R
Names	$c_p(kJ/kgK)$	$c_v(kJ/kgK)$	γ	$c_p - c_v(kJ/kgK)$
Air	1.01	0.718	1.40	0.287
Argon	0.520	0.312	1.667	0.208
carbon monoxide	1.02	0.72	1.40	0.297
carbon dioxide	0.844	0.655	1.289	0.189
Helium	5.19	3.12	1.667	2.08
Hydrogen	14.32	10.16	1.405	4.12
Methane	2.22	1.70	1.304	0.518
Neon	1.03	0.618	1.667	0.412
Nitrogen	1.04	0.743	1.4	0.297

Table 5.3: Specific heats and ratio of specific heats of gases [42].

Gas	Temperature (C)	Speed of sound (m/s)
Air	0	331.5
Air	20	344
Air	50	360.3
Argon	0	307.85
Helium	0	972
Helium	20	927
Hydrogen	0	1270
Carbon dioxide	0	260
Carbon monoxide	0	336
Neon	30	461
Nitrogen	29	354.4

Table 5.4: Speed of sound in ideal gases.

Appendix B

MATLAB code to solve non-linear ODE

function $shooting_reviewandersson$ global XSTART XSTOP H Pr

$XSTART = 0; XSTOP = 14; Pr = 2; H = 0.1; freq = 1;$

$u = [-1 \quad -1];$

$x = XSTART;$

$u = newtonRaphson2(@residual, u);$

$[xSol, ySol] = runKut5(@dEqs, x, inCond(u), XSTOP, H);$

printSol(xSol,ySol,freq)

result = -ySol(1,3)

plot(xSol, ySol(:,2))

$function F = dEqs(x, y)$

global Pr

My equations for compressible laminar boundary layer over a stretching sheet- Andersson's paper

$\quad yy1 = y(2)^2 - y(1) * y(3);$

$yy2 = -Pr * y(1) * y(5);$

$F = zeros(1, 5);$

$F(1) = y(2);$

$F(2) = y(3);$

$F(3) = yy1;$

$F(4) = y(5);$

$F(5) = yy2;$

ysol = [y(2); y(3); yy1; y(5); yy2]; $function y = inCond(u)$

$y = [0 \quad 1 \quad u(1) \quad 1 \quad u(2)];$

$function r = residual(u)$

global XSTART XSTOP H

$r = zeros(length(u), 1);$

$x = XSTART;$

$[xSol, ySol] = runKut5(@dEqs, x, inCond(u), XSTOP, H);$

$lastRow = size(ySol, 1);$

$r(1) = ySol(lastRow, 2);$

$r(2) = ySol(lastRow, 4);$

Subroutines for the Shooting Method

Subroutine of Newton-Raphson method

$function root = newtonRaphson2(func, x, tol)$

$if nargin == 2; tol = 1.0e4 * eps;$ end

$if size(x, 1) == 1; x = x';$ end

$for i = 1 : 10$

$[jac, f0] = jacobian(func, x);$

$if sqrt(dot(f0, f0)/length(x)) < tol$

$root = x;$ return

end

$dx = (jac)/(-f0);$

$x = x + dx;$

$if sqrt(dot(dx, dx)/length(x)) < tol * max(abs(x), 1.0)$

$root = x;$ return

end

disp(i)

end

error('Too many iterations')

$function [jac, f0] = jacobian(func, x)$

$h = 1.0e - 4;$

$n = length(x);$

$jac = zeros(n);$

$f0 = feval(func, x);$

$$for\, i = 1 : n$$
$$temp = x(i);$$
$$x(i) = temp + h;$$
$$f1 = feval(func, x);$$
$$x(i) = temp;$$
$$jac(:, i) = (f1 - f0)/h;$$
end

Subroutine of Runge-Kutta method.

$$function[xSol, ySol] = runKut5(dEqs, x, y, xStop, h, eTol)$$

if size(y,1) ¿ 1 ;$y = y'$; end $if\, nargin < 6; eTol = 1.0e - 6;$ end

$$n = length(y);$$
$$A = [0\, 1/5\, 3/10\, 3/5\, 1\, 7/8];$$

$$B = [0\ 0\ 0\ 0\ 0\ 1/5\ 0\ 0\ 0\ 0\ 3/40\ 9/40\ 0\ 0\ 0\ 3/10\ -9/10\ 6/5\ 0\ 0$$
$$\quad -11/54\ 5/2\ -70/27\ 35/27\ 0\ 1631/55296\ 175/51\ 575/13824\ 44275/110592\ 253/4096];$$

$$C = [37/378\ 0\ 250/621\ 125/594\ 0\ 512/1771];$$
$$D = [2825/27648\ 0\ 18575/48384\ 13525/55296\ 277/14336\ 1/4];$$
$$xSol = zeros(2, 1); ySol = zeros(2, n);$$
$$xSol(1) = x; ySol(1, :) = y;$$
$$stopper = 0; k = 1;$$
$$for\, p = 2 : 5000$$
$$K = zeros(6, n);$$
$$K(1, :) = h * feval(dEqs, x, y);$$
$$for\, i = 2 : 6$$
$$BK = zeros(1, n);$$
$$for\, j = 1 : i - 1$$
$$BK = BK + B(i, j) * K(j, :);$$
end
$$K(i, :) = h * feval(dEqs, x + A(i) * h, y + BK);$$
end
$$dy = zeros(1, n); E = zeros(1, n);$$

$for\, i = 1 : 6$

$dy = dy + C(i) * K(i, :);$

$E = E + (C(i) - D(i)) * K(i, :);$

end

$e = sqrt(sum(E. * E)/n);$

$if\, e <= eTol$

$y = y + dy; x = x + h;$

$k = k + 1;$

$xSol(k) = x; ySol(k, :) = y;$

$if\, stopper == 1;$

break

end

end

$if\, e = 0; hNext = 0.9 * h * (eTol/e)^0.2;$

else;

$hNext = h;$ end

$if (h > 0) == (x + hNext >= xStop)$

$hNext = xStop - x; stopper = 1;$

end

$h = hNext;$

end

Chapter 2 (bvp4c Codes)

This MATLAB program of chapter 3 to find the solution of compressible fluid over a linearly stretching sheet using bvp4c method.

$function\ bvp4c_extension A$

clear all

close all

$Pr = 0.7;$

$function\, ysol = bvpex1(x, y)$

$yy1 = y(2)^2 - y(1) * y(3);$

$yy2 = -Pr * y(1) * y(5);$

$ysol = [y(2); y(3); yy1; y(5); yy2];$

end $functionres = bcex1(y0, yinf)$

$res = [y0(1); y0(2) - 1; yinf(2); y0(4) - 1; yinf(4)];$

end $sol1 = bvpinit(linspace(0, 32, 26), [10000]);$
$sol = bvp4c(@bvpex1, @bcex1, sol1);$
$x = sol.x;$
$y = sol.y;$
$value = deval(sol, o), 9)$
figure (1) plot(x, y(4, :),'linewidth', 1) $xlabel('\eta')$
$ylabel('\theta(\eta)')$
end

Chapter 3 (bvp4c Codes)

This MATLAB program of chapter 3 to find the effects of temperature-dependent viscosity on heat transfer over a continuous moving surface using bvp4c method.

$function \ bvp4c_extensionB$
clear all
close all
$Pr = 0.7;$
$thetaref = -0.25;$
$functionysol = bvpex1(x, y)$
$yy1 = -(y(3)*j(5))/(thetaref - y(4)) - (y(1)*y(3) - y(2)^2)*(thetaref - y(4))/thetaref;$
$yy2 = -Pr * y(1) * y(5);$
$ysol = [y(2); y(3); yy1; y(5); yy2];$
end
$functionres = bcex1(y0, yinf)$
$res = [y0(1); y0(2) - 1; yinf(2); y0(4) - 1; yinf(4)];$
end
$sol1 = bvpinit(linspace(0, 32, 26), [1 \quad 0 \quad 0 \quad 0 \quad 0]);$

```
sol = bvp4c(@bvpex1, @bcex1, sol1);
x = sol.x;
y = sol.y;
figure(1)
plot(x, y(2, :)
xlabel('η')
ylabel('df/dη')
end
end
```